Supporting information for

Calix[4]pyrrole Bis-crowns as Ion Pair Receptors: Cation Selectivity

Modulated by the Counter Anions

Ju Ho Yang,[#] Ju Hyun Oh,[#] Seung-Ryong Kwon and Sung Kuk Kim[*]

Department of Chemistry and Research Institute of Natural Science, Gyeongsang National University, Jinju, 660-701, Korea

1. General experimental and synthetic details

Solvents and reagents used for the synthetic work were purchased from Aldrich, TCI, or Alfa Aesar and used without further purification. NMR spectra were recorded on a Bruker Advance-300 MHz instrument. The NMR spectra were referenced to residual solvent peaks and the spectroscopic solvents were purchased from either Cambridge Isotope Laboratories or Aldrich. Fast atom bombardment (FAB) mass spectra (MS) were recorded on a JMS-700 (JEOL) spectrometer. TLC analyses were carried out using Sorbent Technologies silica gel (200 mm) sheets. Column chromatography was performed on Sorbent silica gel 60 (40–63 mm). Calix[4]pyrrole **5** was synthesized following a literature procedure.[1,2] The X-ray crystallographic analysis was carried out on a Rigaku Oxford Diffraction HyPix6000E Synergy diffractometer using a μ-focus Cu Kα radiation source (λ = 1.5418 Å) with collimating mirror monochromators.

Compound 2

To acetonitrile (100 mL) were added calix[4]pyrrole **6** (1.00 g, 1.34 mmol) and triethylene glycol ditosylates (1.23 g, 2.68 mmol) in the presence of 12 equiv of K_2CO_3 (2.23 g). The reaction mixture was stirred under a nitrogen atmosphere for 3 days at reflux. After the reaction was completed, the volatile solvent was removed by evaporation *in vacuo*. To the resulting crude reaction mixture, ethyl acetate was added and the organic layer was washed twice with water. The organic layer was separated off and then dried over anhydrous $MgSO_4$. The organic solvent was evaporated in vacuo to give a brownish solid. Column chromatography over neutral alumina (eluent: ethyl acetate/hexane (1:1)) gave receptor **2** (0.13 g, 10% yield) as a white solid. ^{1}H NMR (300 MHz, CDCl$_3$) δ 7.17 (s, 2H), 7.04 (s, 2H), 6.89 – 6.79 (m, 8H), 6.73 – 6.63 (m, 8H), 6.09 (d, J = 2.5 Hz, 4H), 6.00 (d, J = 2.6 Hz, 4H), 4.10 – 4.00 (m, 8H), 3.93 – 3.78 (m, 8H), 3.74 (s, 8H), 1.90 (s, 12H). ^{13}C NMR (75 MHz, chloroform-*d*) δ 157.1, 137.3, 136.6, 128.4, 113.7, 106.1, 105.2, 71.1, 69.7, 67.4, 44.0, 30.1 ppm. HRMS (FAB) *m/z* 969.4825 [M + H$^+$] calc. for $C_{60}H_{65}N_4O_8$, found 969.4802.

Compound 3

To acetonitrile (100 mL) were added calix[4]pyrrole **6** (1.00 g, 1.34 mmol) and tetraethylene glycol ditosylates (1.42 g, 2.82 mmol) in the presence of 12 equiv of K_2CO_3 (2.23 g). The reaction mixture was stirred under a nitrogen atmosphere for 3 days at reflux. After the reaction was completed, the volatile solvent was removed by evaporation *in vacuo*. To the resulting crude reaction mixture, ethyl acetate was added, and the organic layer was washed twice with water. The organic layer was separated off and then dried over anhydrous $MgSO_4$. The organic solvent was evaporated in vacuo to give a brownish solid. Column chromatography over silica gel (eluent: ethyl acetate/hexane (3:2)) gave receptor **3** (0.33 g, 23% yield) as a white solid. ^{1}H NMR (300 MHz, CDCl$_3$) δ 7.59 (s, 2H), 7.34 (s, 2H), 6.83 (d, J = 8.7 Hz, 8H), 6.64 (d, J = 8.6 Hz, 8H), 6.02 (d, J = 2.5 Hz, 4H), 5.67 (s, 4H), 4.09 – 3.95 (m, 8H), 3.79 (t, J = 4.9 Hz, 8H), 3.70 – 3.55 (m, 16H), 1.84 (s, 12H). ^{13}C NMR (75 MHz, chloroform-*d*) δ 156.1, 136.1, 127.5, 112.6, 104.5, 69.6, 68.4, 66.4, 43.0 ppm. HRMS (FAB) *m/z* 1057.5326 [M + H$^+$] calc. for $C_{64}H_{73}N_4O_{10}$, found 1057.5327.

Compound 4

To acetonitrile (100 mL) were added calix[4]pyrrole **6** (1.00 g, 1.34 mmol) and pentaethylene glycol ditosylates (1.47 g, 2.68 mmol) in the presence of 12 equiv of K_2CO_3 (2.23 g). The reaction mixture was stirred under a nitrogen atmosphere for 3 days at reflux. After the reaction was completed, the volatile solvent was removed by evaporation *in vacuo*. To the resulting crude reaction mixture, ethyl acetate was added and the organic layer was washed twice with water. The organic layer was separated off and then dried over anhydrous $MgSO_4$. The organic solvent was evaporated in vacuo to give a brownish solid. Column chromatography over neutral alumina (eluent: ethyl acetate/hexane (1:1)) gave receptor **4** (0.22 g, 15% yield) as a white solid. ^1H NMR (300 MHz, $CDCl_3$) δ 7.81 (s, 2H), 7.47 (s, 2H), 7.02 – 6.93 (m, 8H), 6.80 – 6.70 (m, 8H), 6.10 (d, $J = 2.6$ Hz, 4H), 5.45 (d, $J = 2.5$ Hz, 4H), 4.14 – 4.04 (m, 8H), 3.85 (t, $J = 5.1$ Hz, 8H), 3.76 – 3.62 (m, 24H), 1.93 (s, 12H). ^{13}C NMR (75 MHz, chloroform-*d*) δ 156.1, 136.7, 127.5, 112.5, 104.1, 70.3, 69.0, 68.5, 66.2, 43.0 ppm. HRMS (FAB) *m/z* 1145.5830 [M + H$^+$] calc. for $C_{68}H_{81}N_4O_{12}$, found 1145.5851.

2. ^{1}H NMR spectral data

a) Treatment used where binding between receptors and anions is governed by a binding/release equilibrium that is slow on the NMR time scale:

Equilibrium: $A + B \xrightleftharpoons{K_a} AB$

Equilibrium constant: $K_a = \dfrac{[AB]}{[A][B]} = \dfrac{[AB]}{(c(A) - [AB])(c(B) - [AB])}$ (1)

$c(A)$ and $c(B)$ are the initial concentrations of A and B, and [A], [B] and [AB] are the equilibrium concentrations of the three species.

A and B is in slow exchange with the complex AB on the ^{1}H NMR time scale.

Two signals for one specific proton on A can be seen in the spectrum, corresponding to complexed and uncomplexed forms of A:
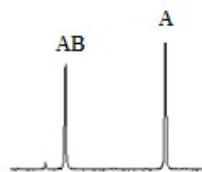
Single-point Methods

K_a is determined from the integrals of complexed and uncomplexed A. If $I(A)$ denotes the integral of a signal for one specific proton of A and $I(AB)$ the integral for the same proton in the complex, the concentration of AB at equilibrium is shown by eq 2. The equilibrium expression is obtrained after substituting into eq. (1):

$$[AB] = \frac{I(AB)}{I(A) + I(AB)} c(A)$$ (2)

$$K_a = \frac{\dfrac{I(AB)}{I(A) + I(AB)}}{I(A)\left(c(B) - \dfrac{I(AB)}{I(A) + I(AB)} c(A)\right)}$$ (3)

b) Treatment used where binding between receptors and anions is governed by a binding/release equilibrium that is fast on the NMR time scale:
Binding constants of receptors with anions were calculated using the equation

$y = (b \times x)/(1 + x \times Ka)$, where x = [G], y = $|\delta_0 - \delta|$ (δ is the chemical shift of an indicative receptor proton signal at a certain anion concentration and δ_0 is the chemical shift of the receptor signal for the anion-free form).
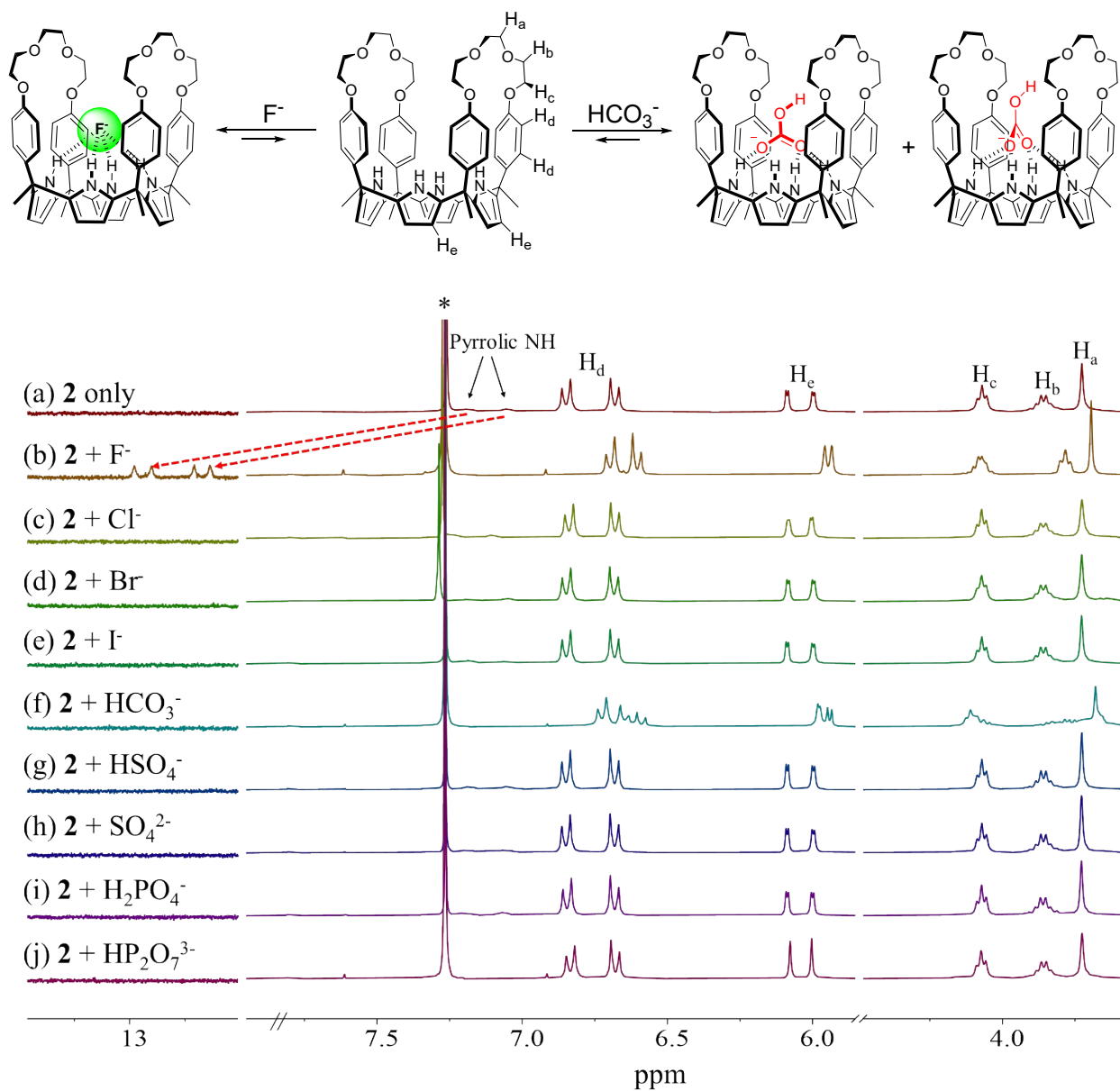
Fig. S1 Top: Proposed binding modes of receptor **2** for F⁻ and HCO₃⁻. Bottom: Partial views of ¹H NMR spectra (300 MHz, 25 °C) of **2** (3 mM) recorded in chloroform-*d* in the presence of the indicated anions (ca. 10 equiv each) as their respective TBA⁺ (tetrabutylammonium) salts except for HCO₃⁻ in the TEA⁺ (tetraethylammonium) salt form. The asterisk (*) denotes a residual NMR solvent peak. The proton signals exhibited at lower fields than δ = 10 ppm were magnified by 2-fold.
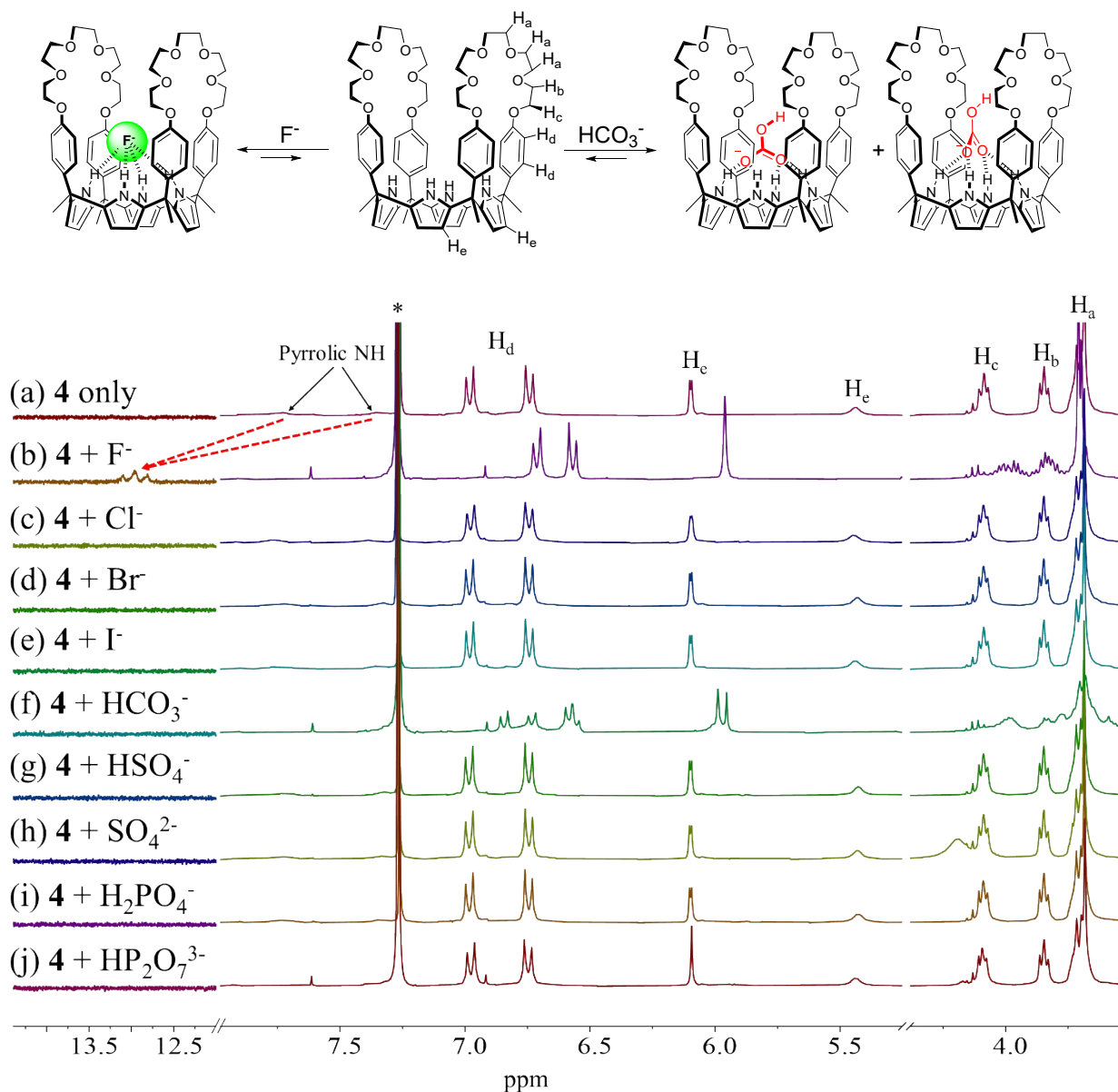
Fig. S2 Top: Proposed binding modes of receptor **4** for F$^-$ and HCO$_3^-$. Bottom: Partial views of ^{1}H NMR spectra (300 MHz, 25 °C) of **4** (3 mM) recorded in chloroform-*d* in the presence of the indicated anions (ca. 10 equiv each) as their respective TBA$^+$ (tetrabutylammonium) salts except for HCO$_3^-$ in the TEA$^+$ (tetraethylammonium) salt form. The asterisk (*) denotes a residual NMR solvent peak. The proton signals exhibited at lower fields than δ = 10 ppm were magnified by 3-fold.

Fig. S3 Partial ^{1}H NMR spectra (300 MHz, 25 °C) recorded during the titration of **2** (3 mM) with TBAF in CDCl$_3$. The asterisk (*) denotes a residual NMR solvent peak. The proton signals exhibited at lower fields than δ = 10 ppm were magnified by 3-fold.

(a) TBAF only

(b) **2** + TBAF
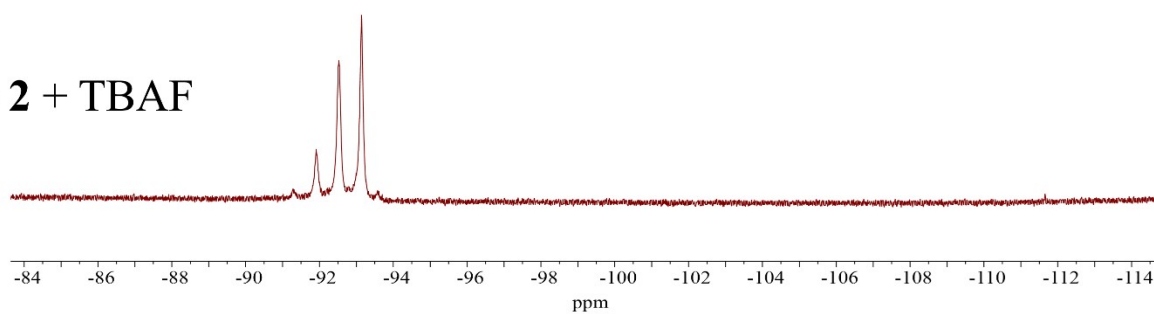
Fig. S4 Partial ^{19}F NMR spectra of (a) TBAF only and (b) receptor **2** (10 mM) + TBAF (5 equiv) recorded in CDCl3. Fluorobenzene was used as an internal reference.
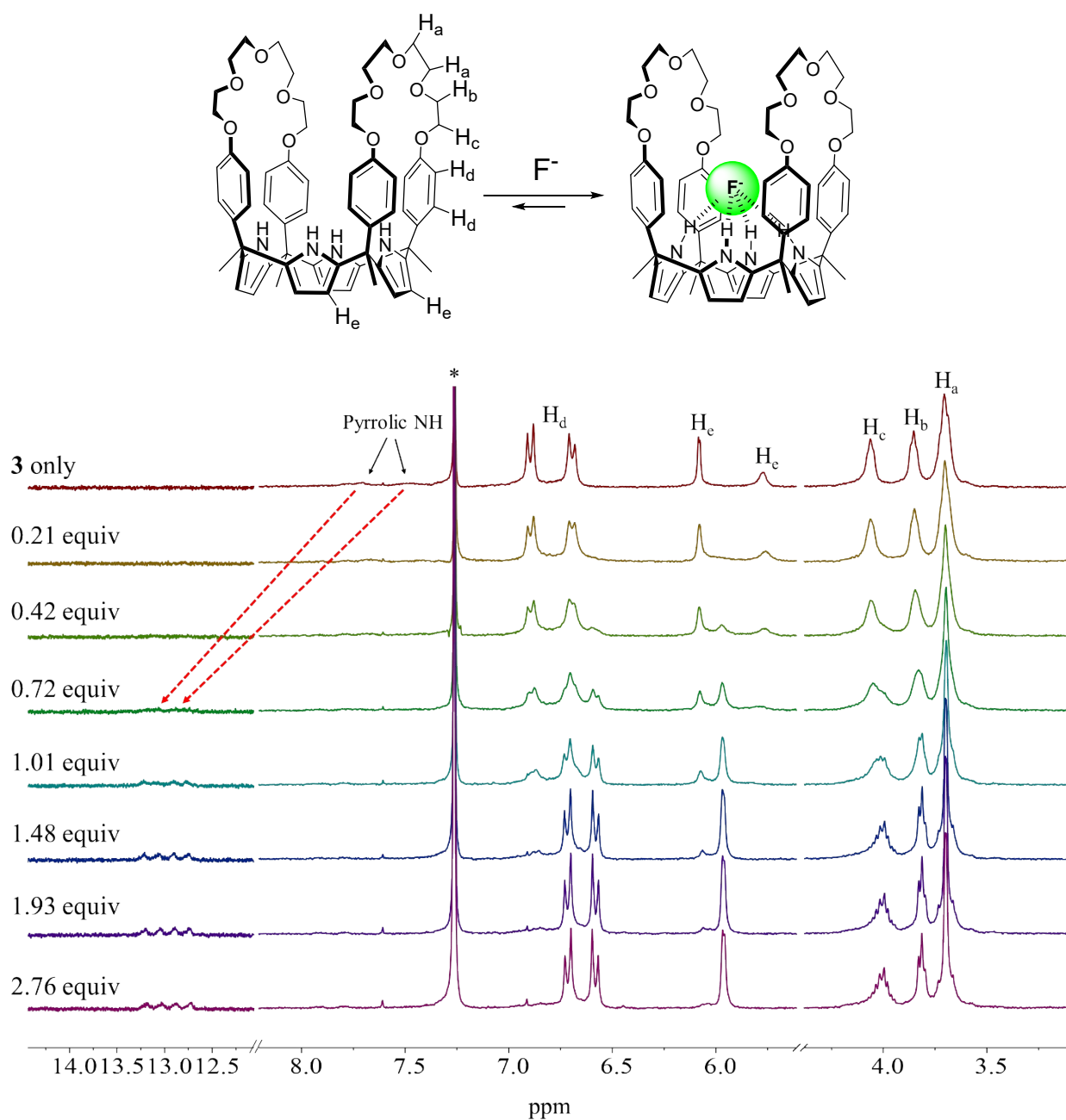
Fig. S5 Partial ^{1}H NMR spectra (300 MHz, 25 °C) recorded during the titration of **3** (3 mM) with TBAF in CDCl$_3$. The asterisk (*) denotes a residual NMR solvent peak. The proton signals exhibited at lower fields than δ = 10 ppm were magnified by 3-fold.

Fig. S6 Partial ^{1}H NMR spectra (300 MHz, 25 °C) recorded during the titration of **4** (3 mM) with TBAF in CDCl$_3$. The asterisk (*) denotes a residual NMR solvent peak. The proton signals exhibited at lower fields than δ = 10 ppm were magnified by 3-fold.

Fig. S7 Top: Two possible binding modes between receptor **2** and HCO_3^-. Bottom: Partial ^1H NMR spectra (300 MHz, 25 °C) recorded during the titration of **2** (3 mM) with $TEAHCO_3$ in $CDCl_3$. The asterisk (*) denotes a residual NMR solvent peak. The proton signals exhibited at lower fields than $\delta = 10$ ppm were magnified by 5-fold.
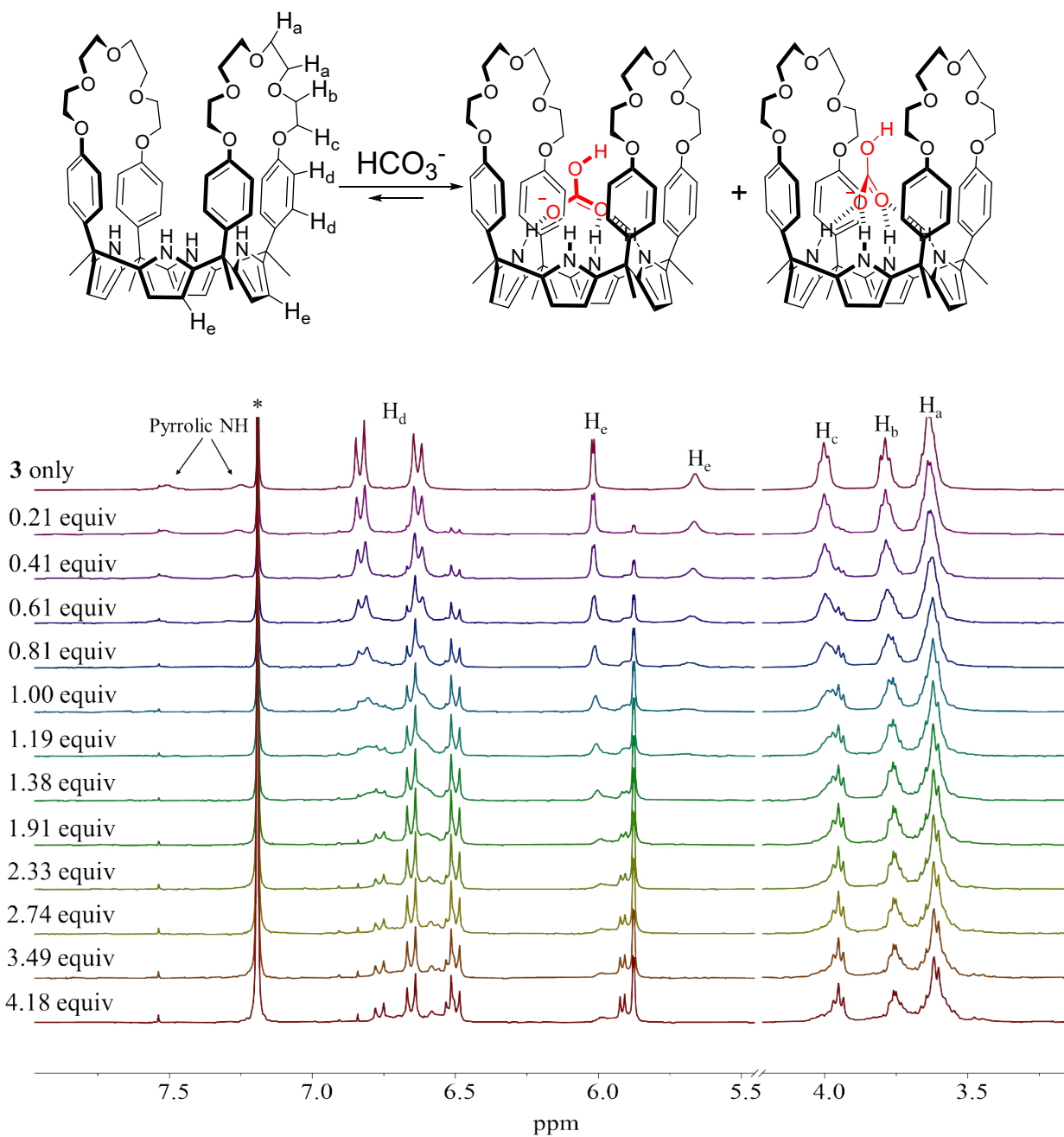
Fig. S8 Top: Two possible binding modes between receptor **3** and HCO_3^-. Bottom: Partial ^{1}H NMR spectra (300 MHz, 25 °C) recorded during the titration of **3** (3 mM) with $TEAHCO_3$ in $CDCl_3$. The asterisk (*) denotes a residual NMR solvent peak.
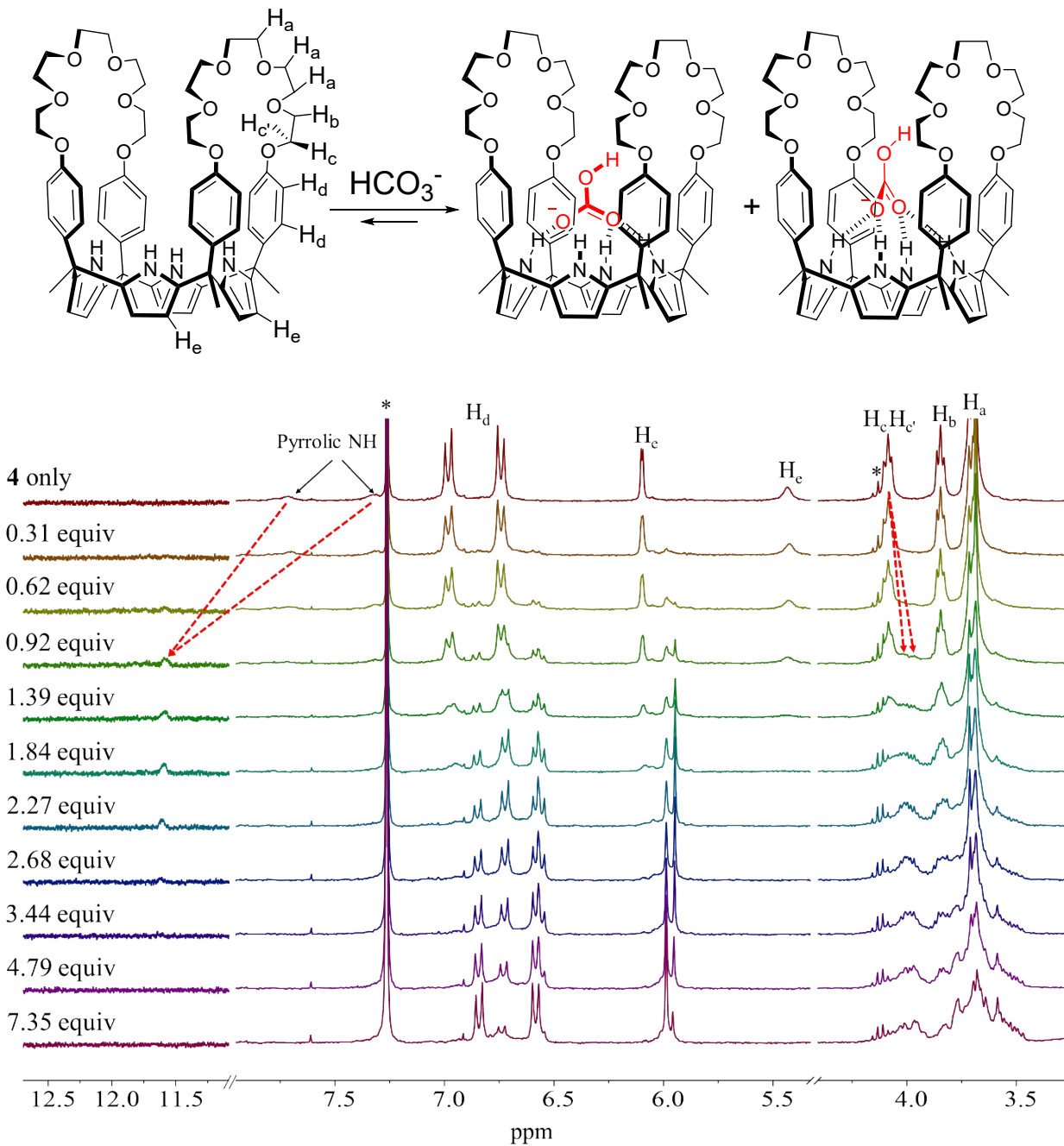
Fig. S9 Top: Two possible binding modes between receptor **4** and HCO_3^-. Bottom: Partial ^{1}H NMR spectra (300 MHz, 25 °C) recorded during the titration of **4** (3 mM) with $TEAHCO_3$ in $CDCl_3$. The asterisk (*) denotes a residual NMR solvent peak.
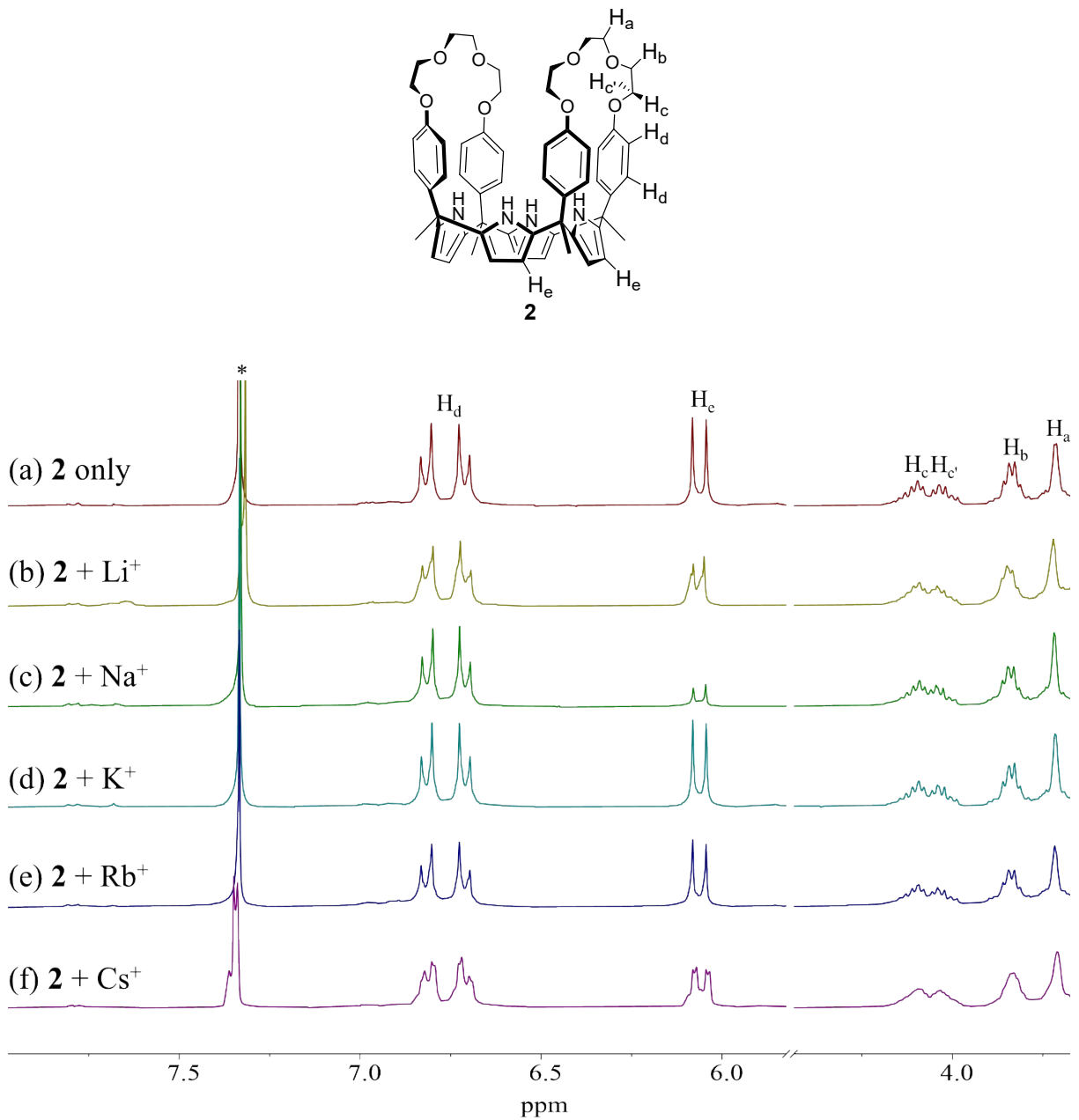
Fig. S10 Partial ^{1}H NMR spectra (300 MHz, 25 °C) of receptor **2** (3 mM) recorded in 10% CD$_3$OD in CDCl$_3$ in the presence of an excess of the indicated alkali metal cations as their respective perchlorate (ClO$_4^-$) salts. The asterisk (*) denotes a residual NMR solvent peak.
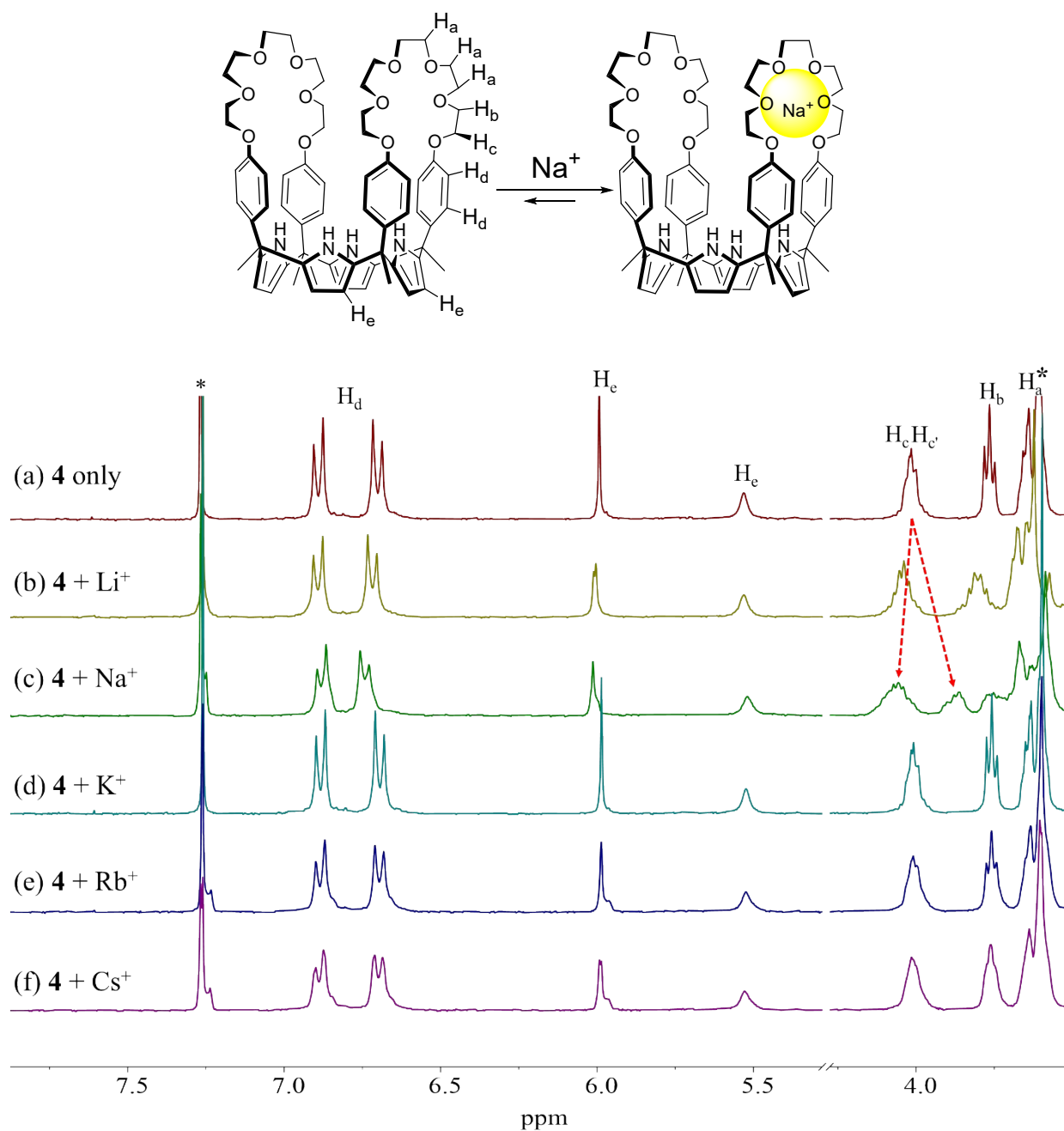
Fig. S11 Top: Proposed binding mode of receptor **4** for Na⁺. Bottom: Partial ¹H NMR spectra (300 MHz, 25 °C) of receptor **4** (3 mM) recorded in 10% CD_3OD in $CDCl_3$ in the presence of an excess of the indicated alkali metal cations as their respective perchlorate (ClO_4^-) salts. The asterisk (*) denotes a residual NMR solvent peak.
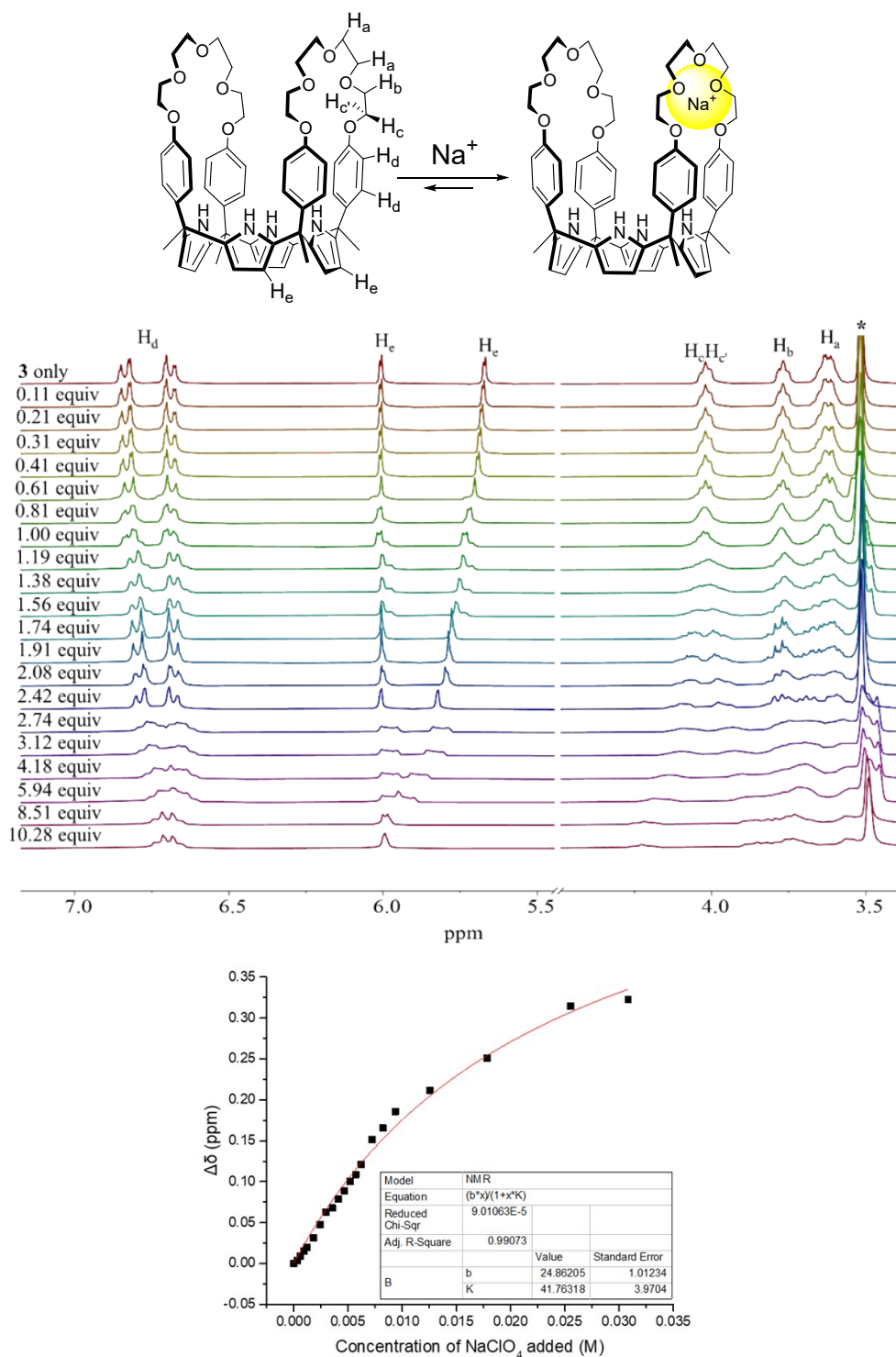
Fig. S12 Partial ^{1}H NMR spectra (300 MHz, 25 °C) recorded during the titration of **3** (3 mM) with NaClO$_4$ in CDCl$_3$:MeOD (9:1, v/v) and the resulting binding isotherm. The asterisk (*) denotes a residual NMR solvent peak.
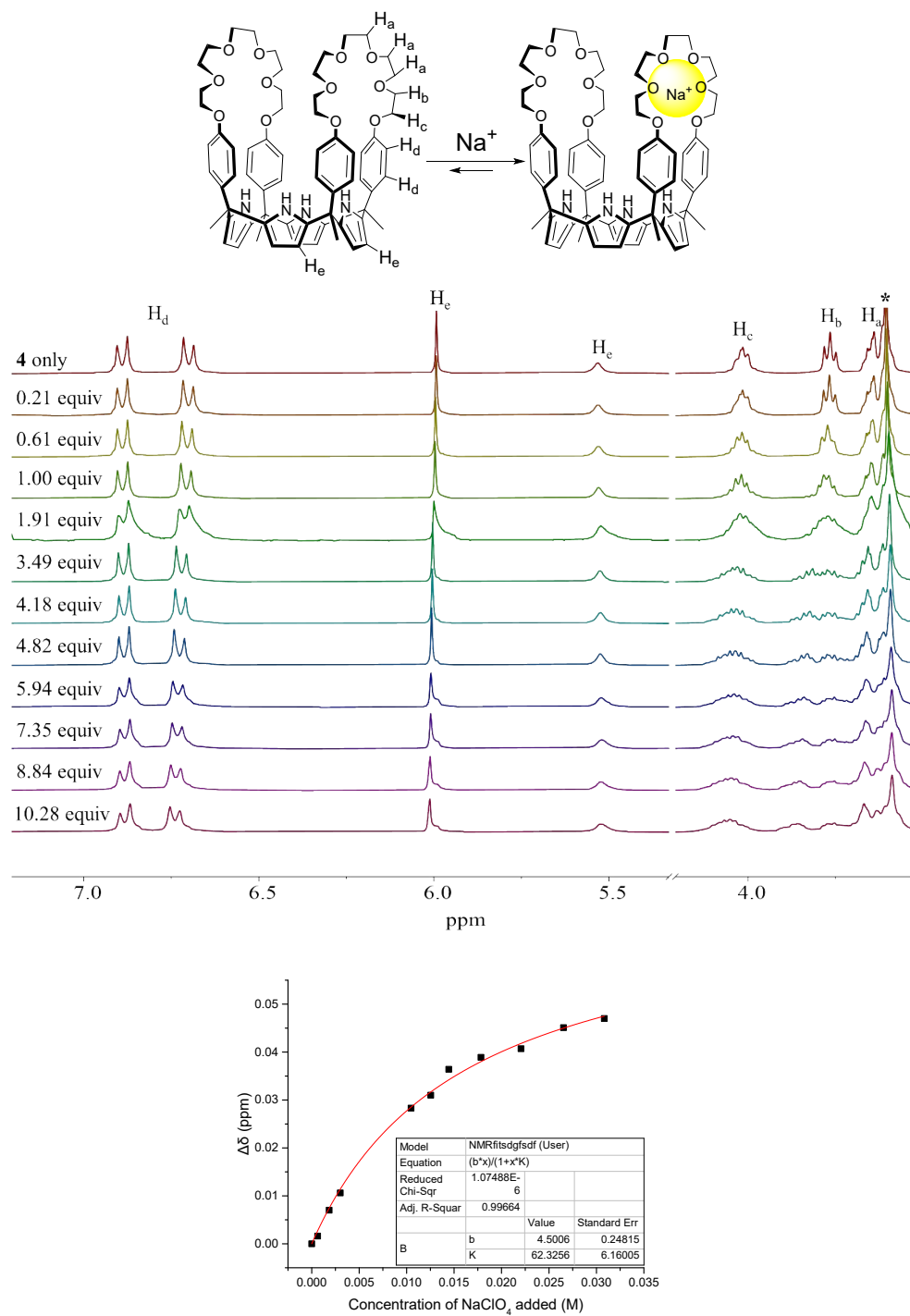
Fig. S13 Partial ^{1}H NMR spectra (300 MHz, 25 °C) recorded during the titration of **4** (3 mM) with NaClO$_4$ in CDCl$_3$:MeOD (9:1, v/v)and the resulting binding isotherm. The asterisk (*) denotes a residual NMR solvent peak.
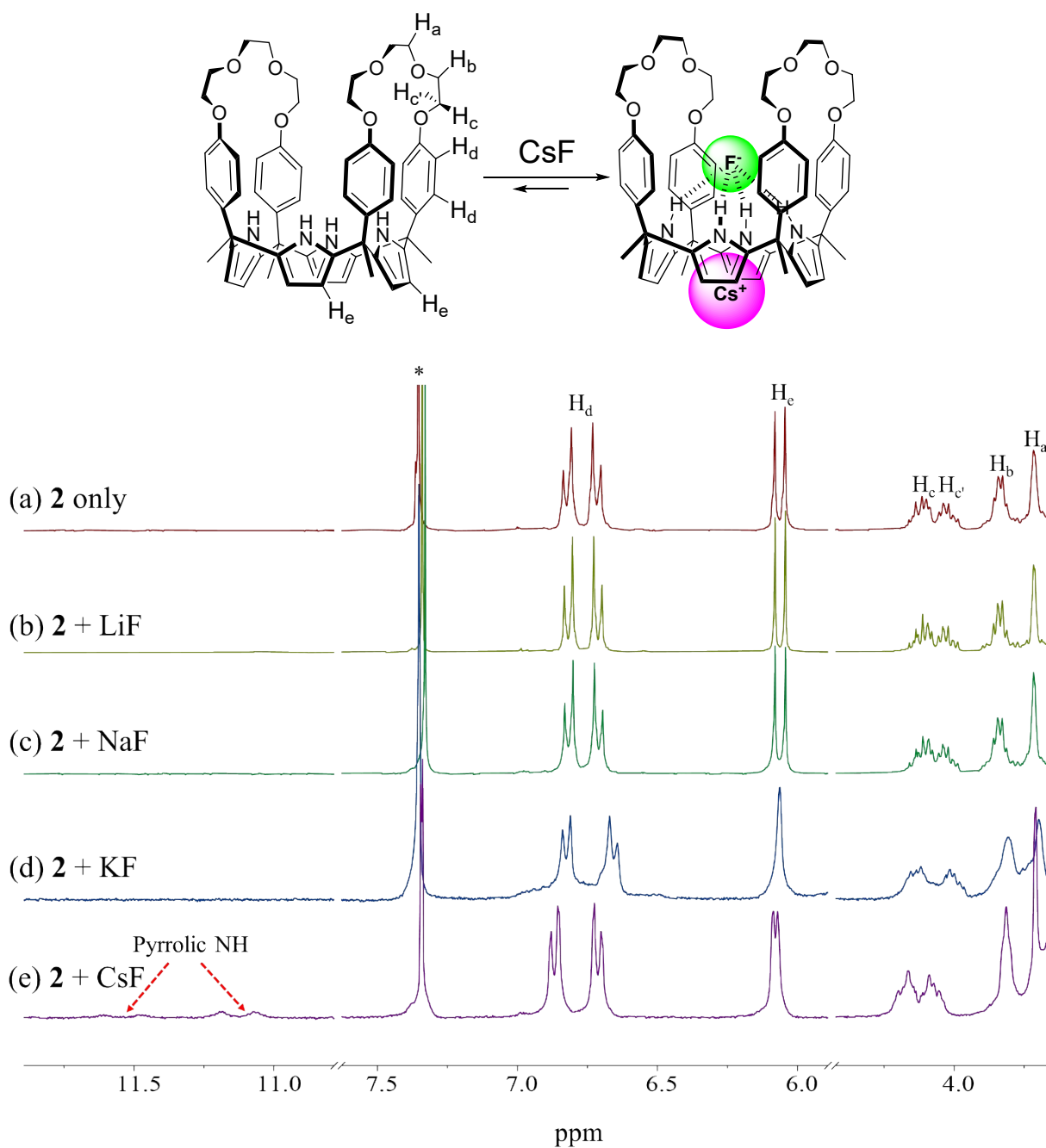
Fig. S14 Top: Putative binding mode of receptor **2** for CsF. Bottom: Partial ^{1}H NMR spectra (300 MHz, 25 °C) of receptor **2** (3 mM) recorded in 10% CD_3OD in $CDCl_3$ in the presence of an excess of the indicated alkali metal fluoride salts. The asterisk (*) denotes a residual NMR solvent peak.
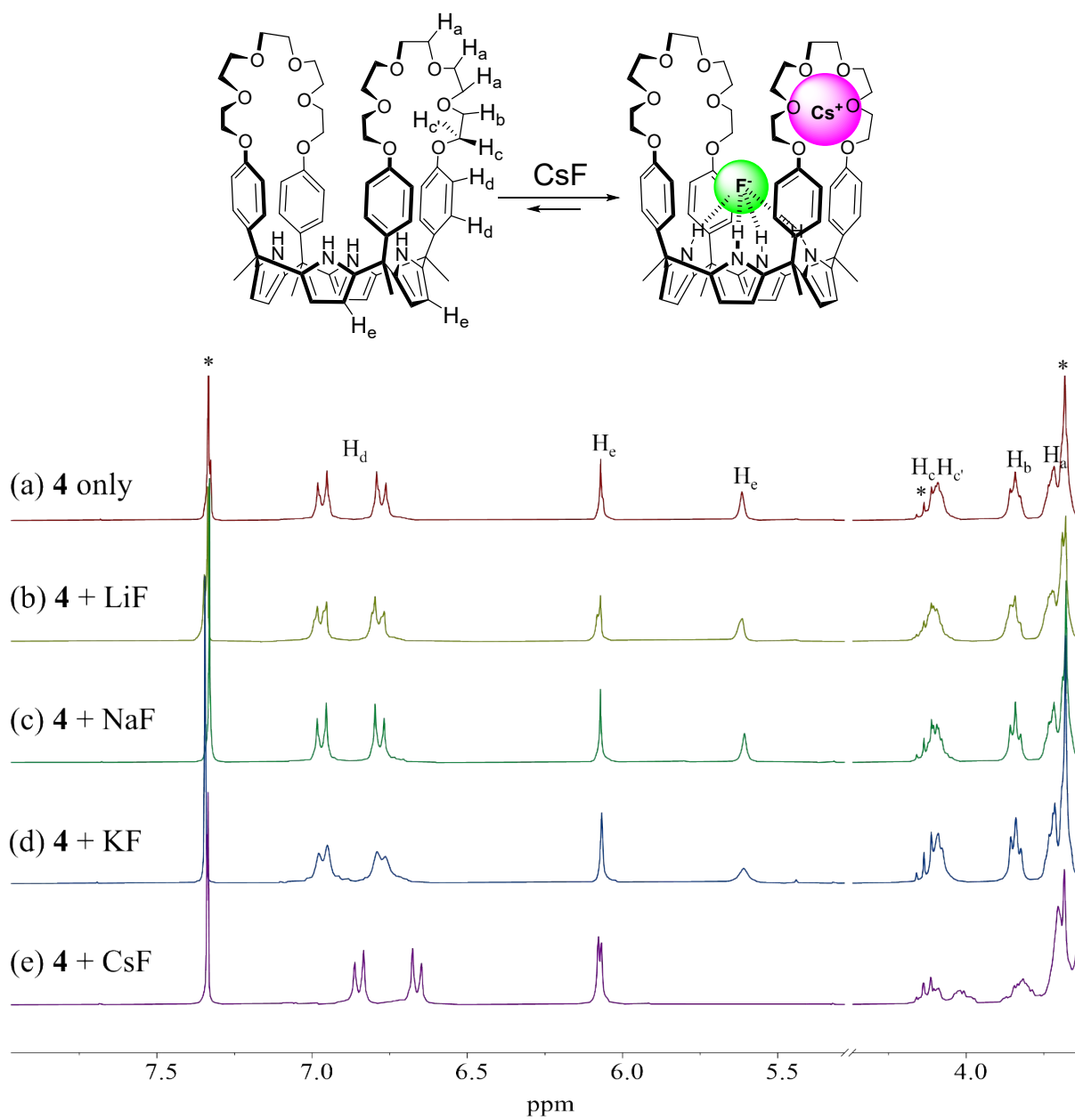
Fig. S15 Top: Putative binding mode of receptor **4** for CsF. Bottom: Partial ^{1}H NMR spectra (300 MHz, 25 °C) of receptor **4** (3 mM) recorded in 10% CD$_3$OD in CDCl$_3$ in the presence of an excess of the indicated alkali metal fluoride salts. The asterisk (*) denotes a residua solvent peak.
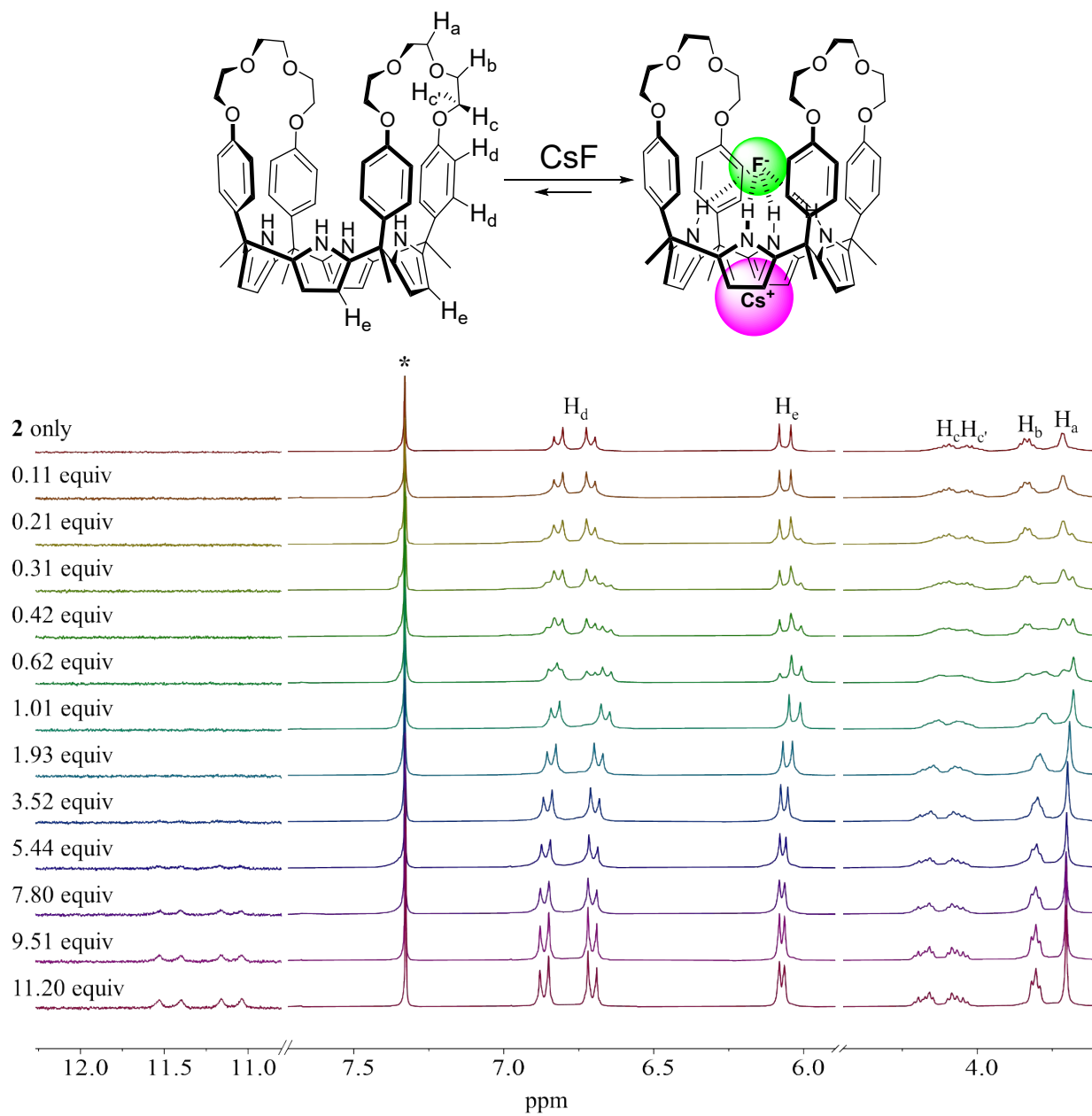
Fig. S16 Partial ^{1}H NMR spectra (300 MHz, 25 °C) recorded during the titration of **2** (3 mM) with CsF in CDCl$_3$:MeOD (9:1, v/v). The asterisk (*) denotes a residual NMR solvent peak.
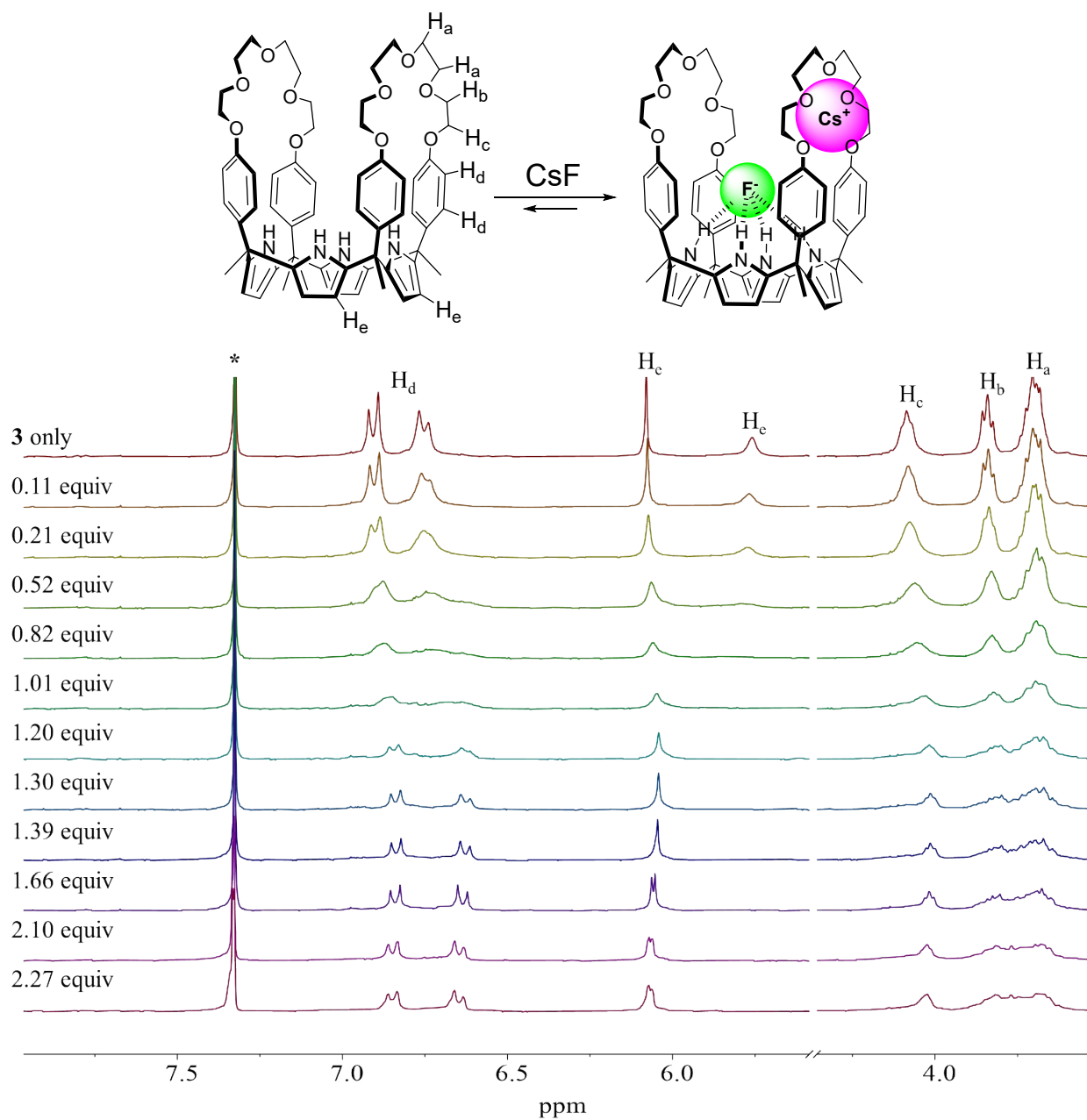
Fig. S17 Partial ^{1}H NMR spectra (300 MHz, 25 °C) recorded during the titration of **3** (3 mM) with CsF in CDCl$_3$:MeOD (9:1, v/v). The asterisk (*) denotes a residual NMR solvent peak.
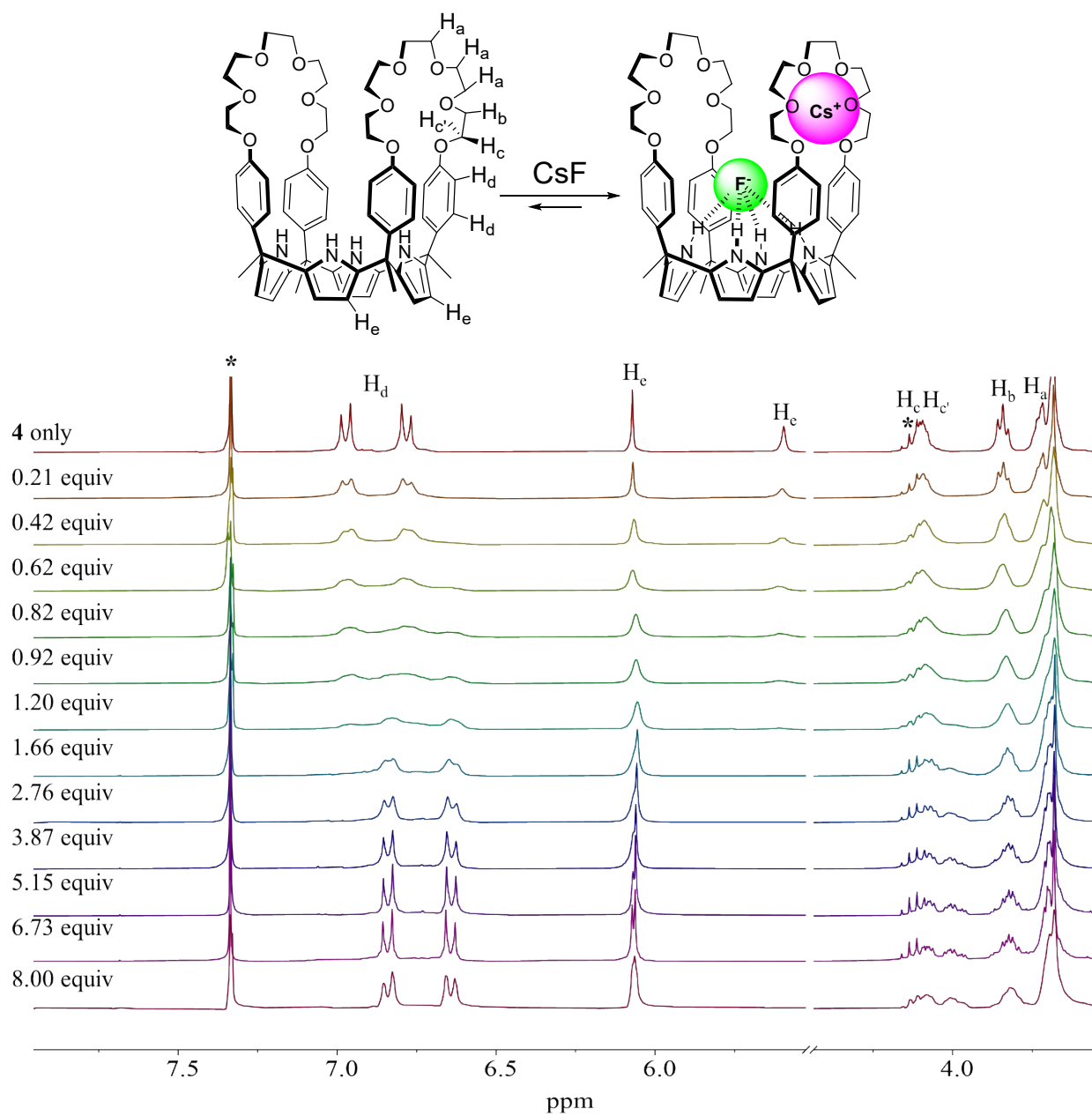
Fig. S18 Partial ^{1}H NMR spectra (300 MHz, 25 °C) recorded during the titration of **4** (3 mM) with CsF in CDCl$_3$:MeOD (9:1, v/v). The asterisks (*) denote a residual solvent peak.
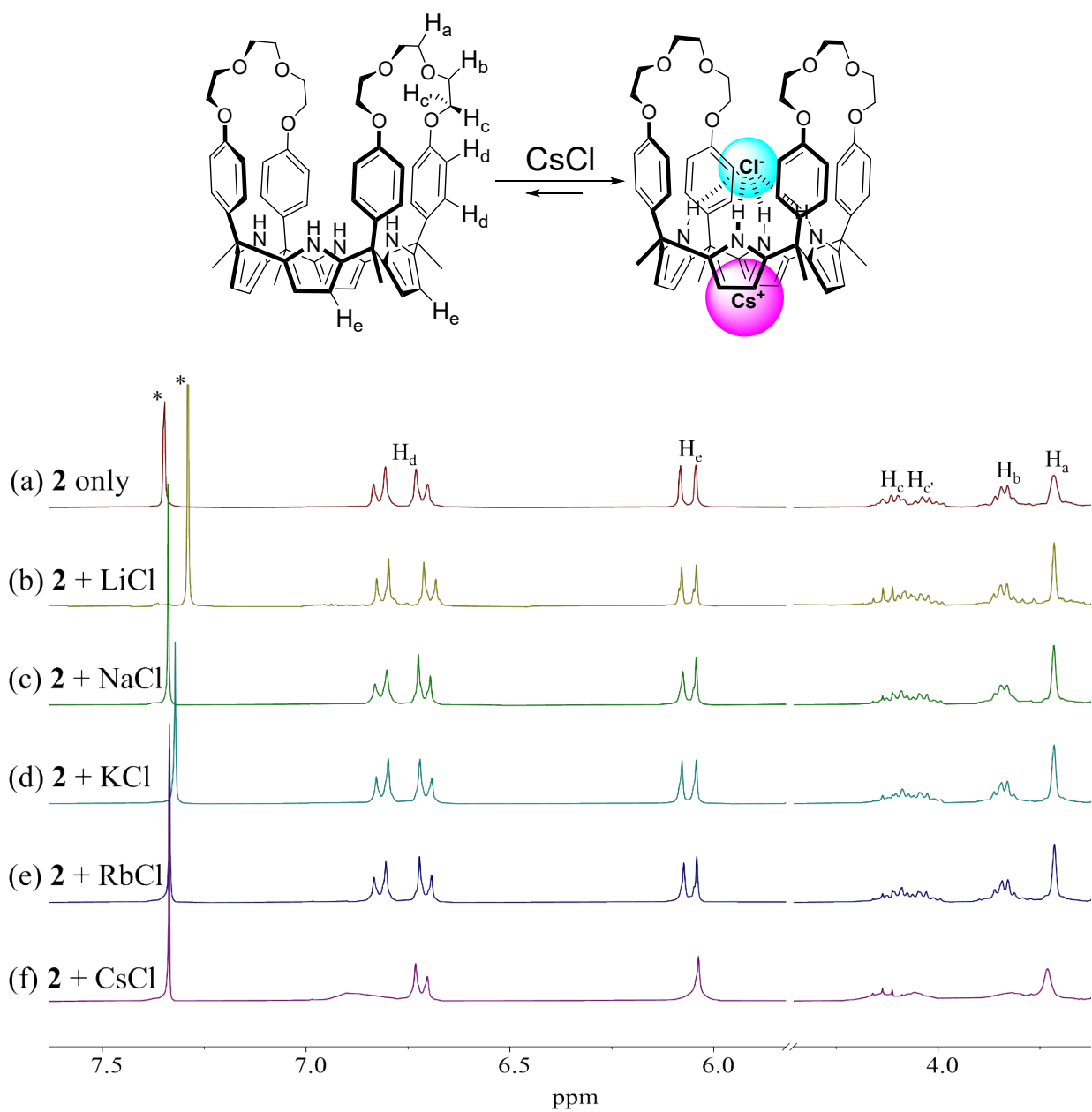
Fig. S19 Top: Putative binding mode of receptor **2** for CsCl. Bottom: Partial ^{1}H NMR spectra (300 MHz, 25 °C) of receptor **2** (3 mM) recorded in 10% CD$_3$OD in CDCl$_3$ in the presence of an excess of the indicated alkali metal chloride salts. The asterisk (*) denotes a residual NMR solvent peak.
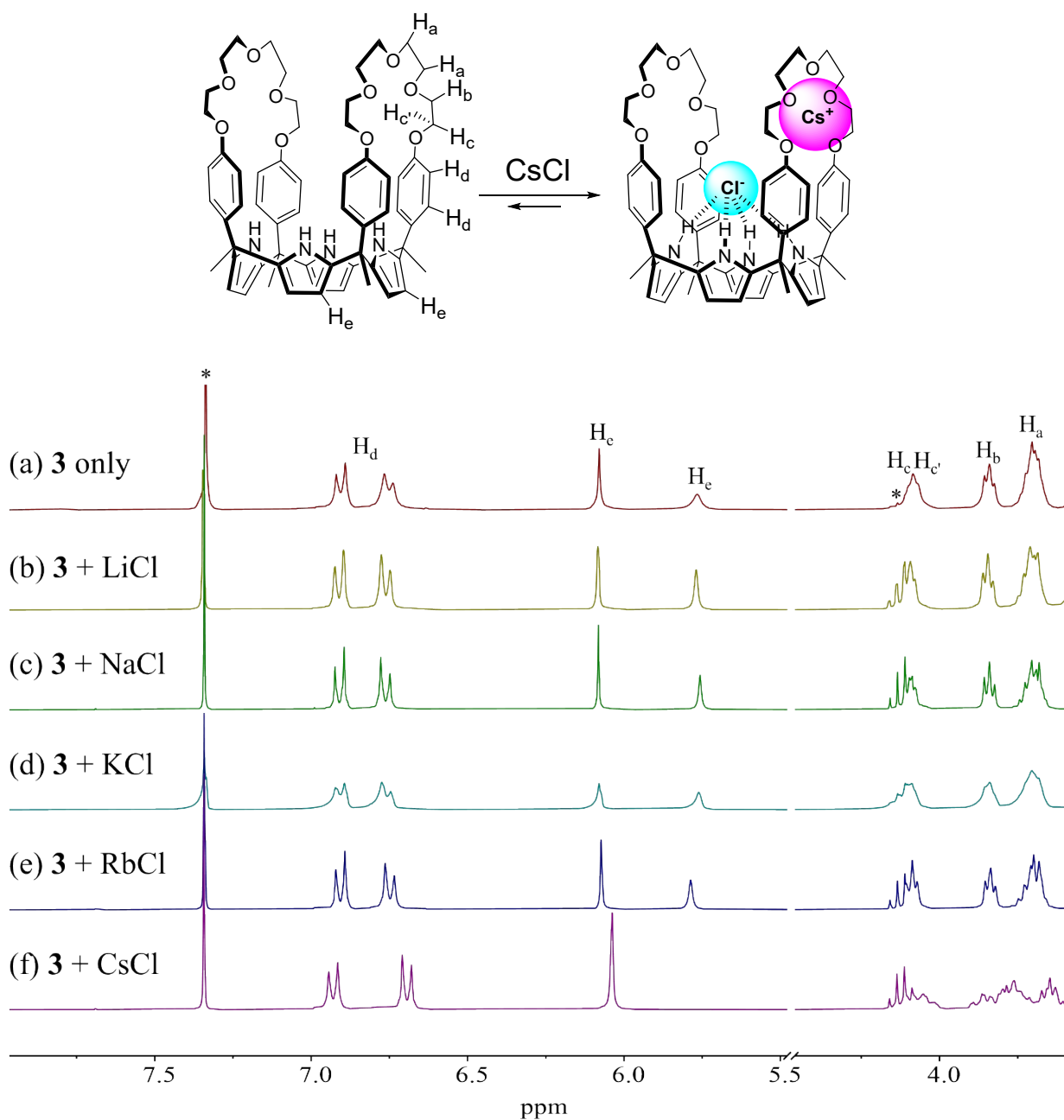
Fig. S20 Top: Putative binding mode of receptor **3** for CsCl. Bottom: Partial ^{1}H NMR spectra (300 MHz, 25 °C) of receptor **3** (3 mM) recorded in 10% CD$_3$OD in CDCl$_3$ in the presence of an excess of the indicated alkali metal chloride salts. The asterisks (*) denotes residual solvent peaks.
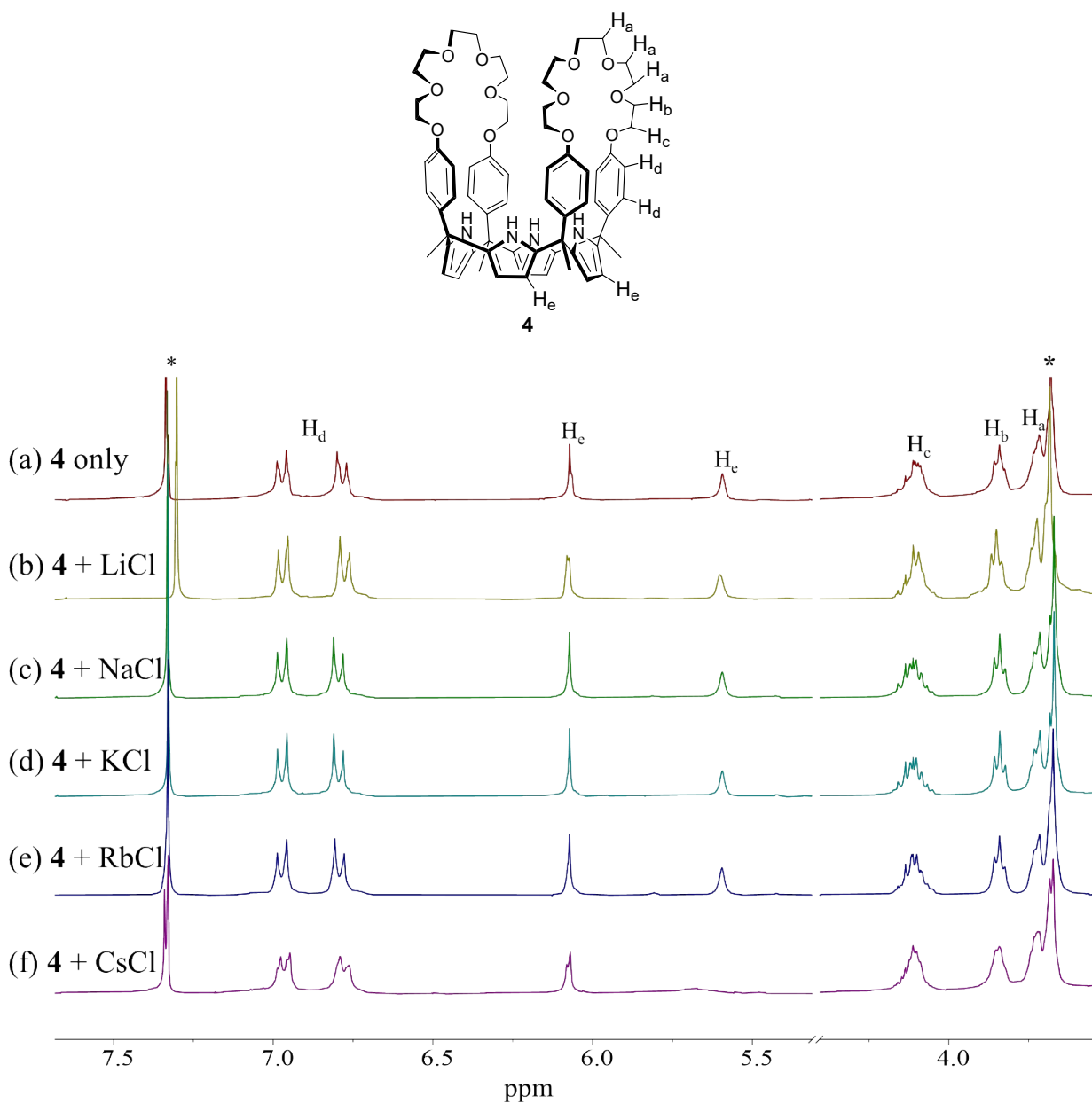
Fig. S21 Partial ^{1}H NMR spectra (300 MHz, 25 °C) of receptor **4** (3 mM) recorded in 10% CD$_3$OD in CDCl$_3$ in the presence of an excess of the indicated alkali metal chloride salts. The asterisk (*) denotes residual solvent peaks.
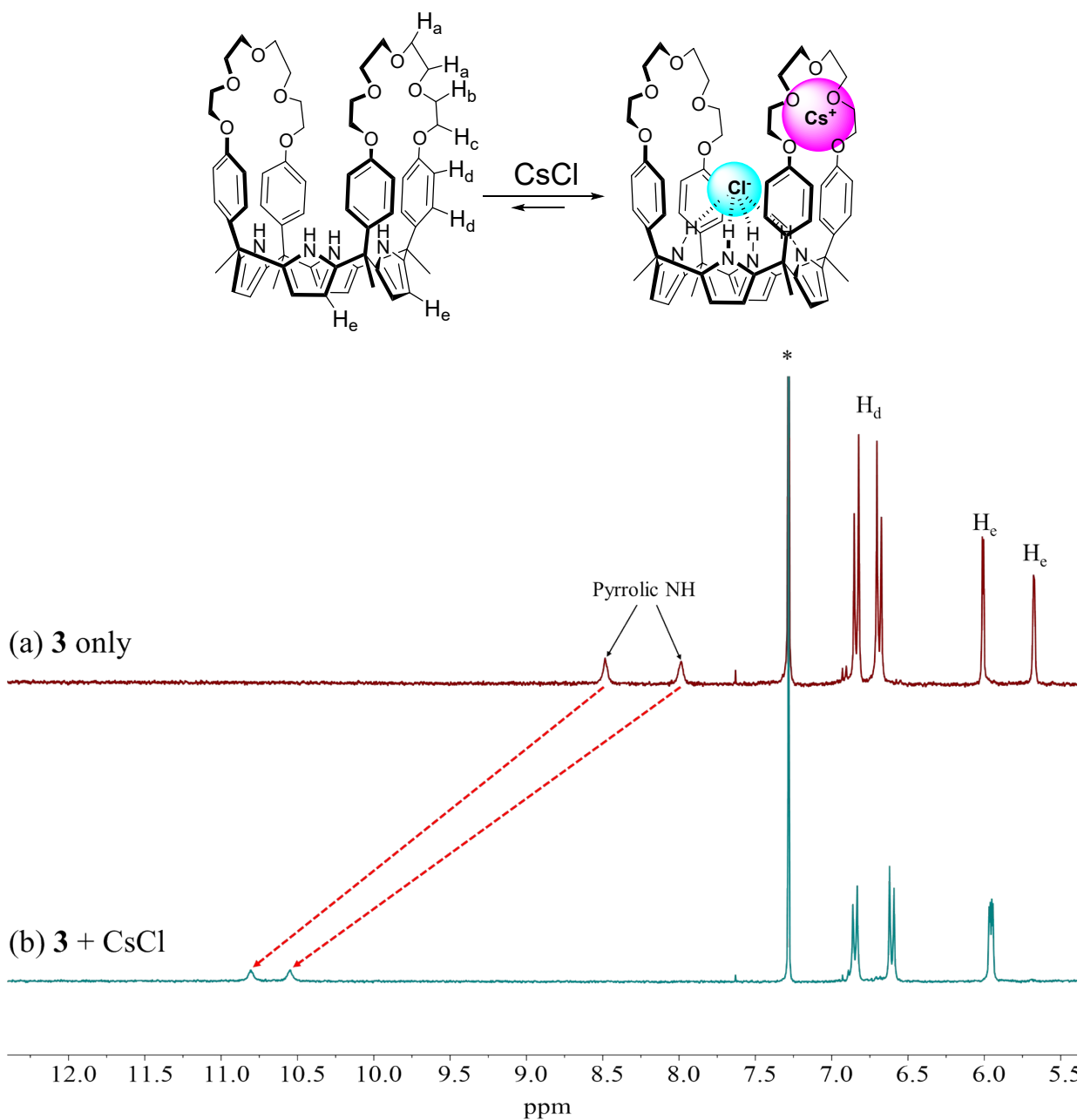
Fig. S22 Partial ^{1}H NMR spectra (300 MHz, 25 °C) of receptor **3** (3 mM) recorded in 10% CH$_3$OH in CDCl$_3$ in the presence of an excess of the indicated cesium chloride salts. The asterisk (*) denotes residual solvent peaks.
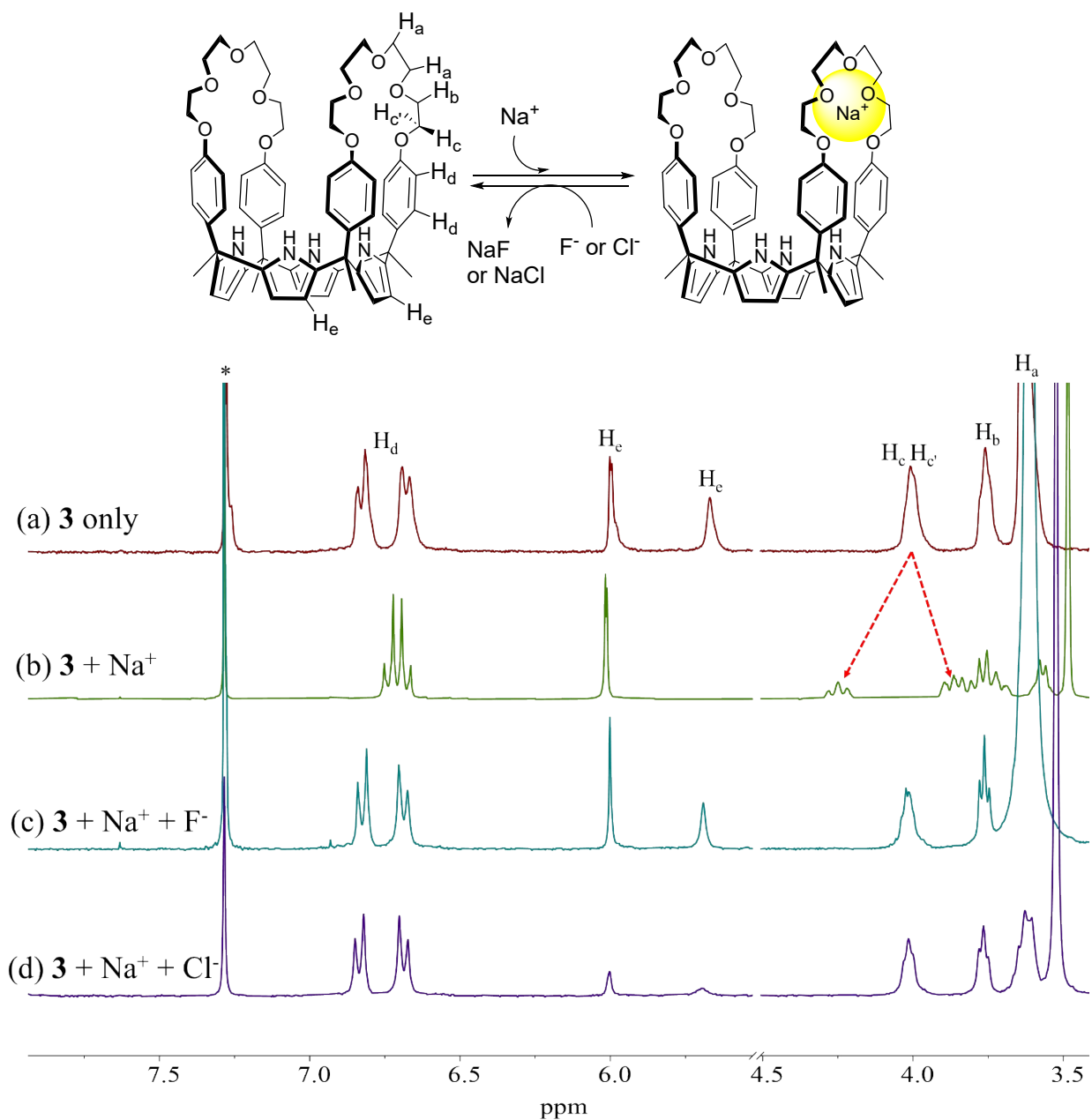
Fig. S23 Top: Proposed binding behavior of receptor **3** for Na$^+$ in the absence and presence of F$^-$ and Cl$^-$. Bottom: Partial ^{1}H NMR spectra (300 MHz, 25 °C) of (a) **3** (3 mM) only, (b) **3** + excess NaClO$_4$, (c) **3** + excess NaClO$_4$ + excess TBAF, (d) **3** + excess NaClO$_4$ + excess TBACl in 10% CD$_3$OD in CDCl$_3$. The asterisk (*) denotes a residual NMR solvent peak.
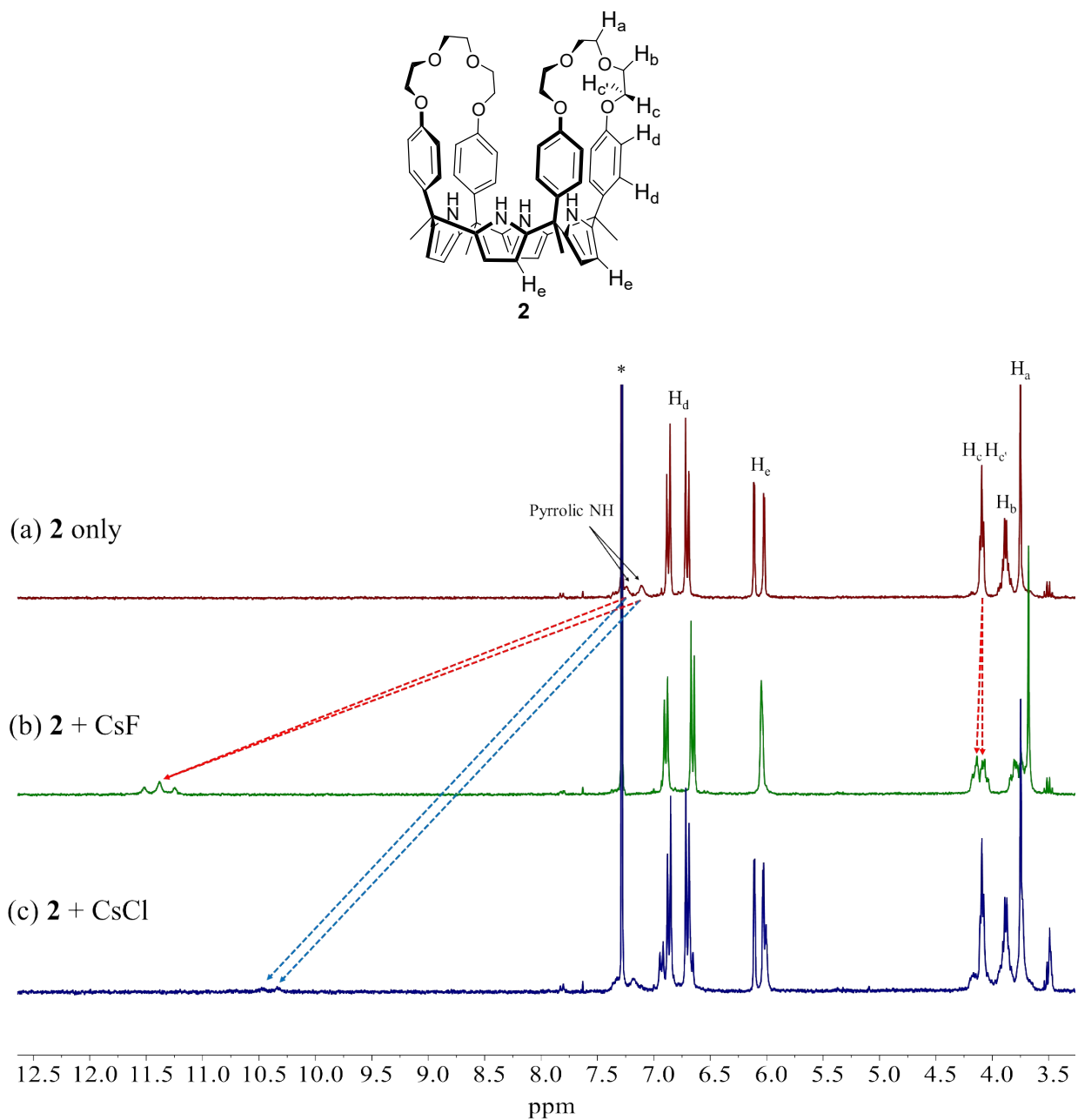
Fig. S24 Partial ^{1}H NMR spectra (300 MHz, 25 °C) of receptor **2** (3 mM) before and after the addition of solid CsF (5.0 equiv) and CsCl (5.0 equiv) in CDCl$_3$. The asterisk denotes a residual NMR solvent peak.
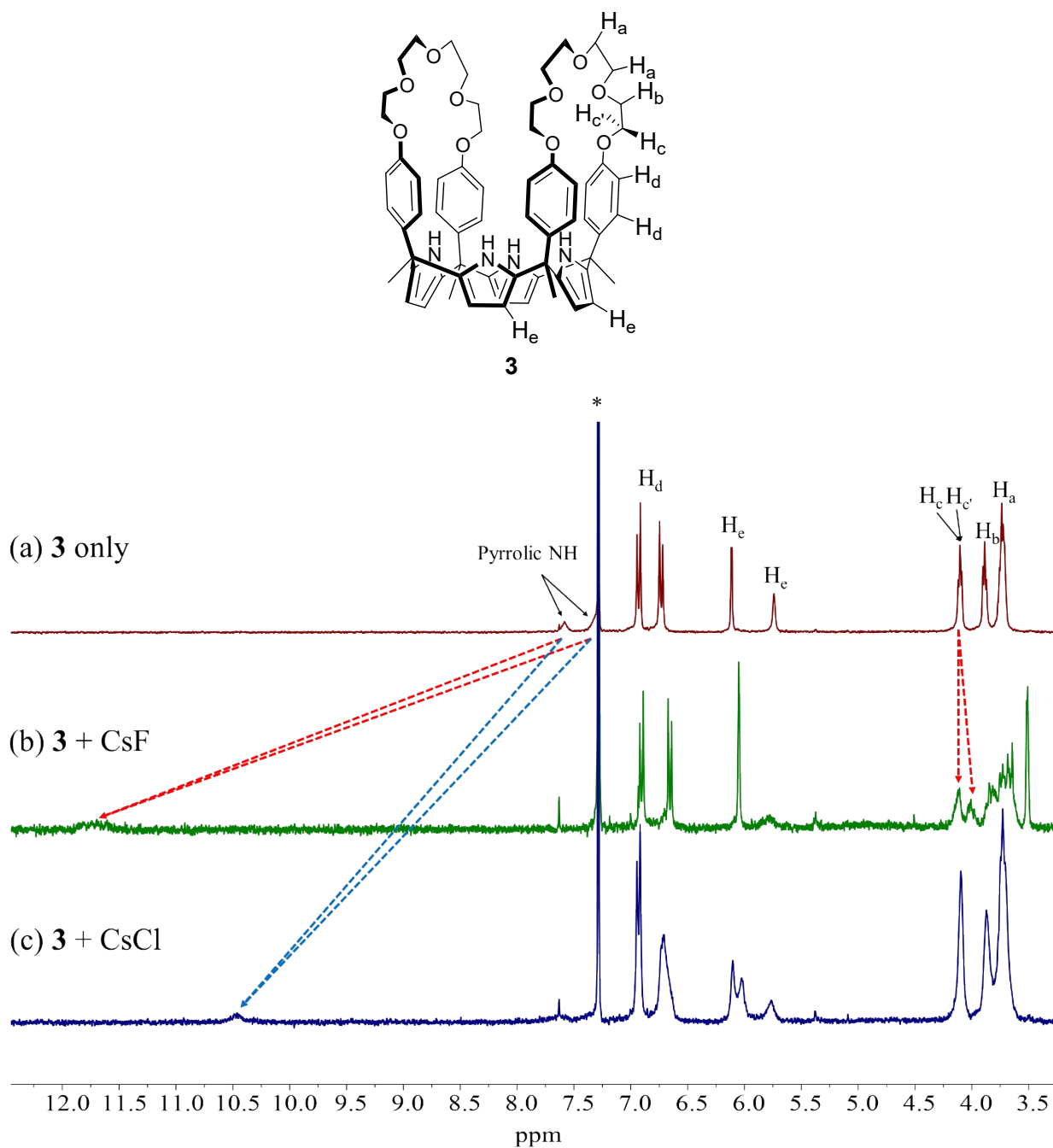
Fig. S25 Partial ^{1}H NMR spectra (300 MHz, 25 °C) of receptor **3** (3 mM) before and after the addition of solid CsF (5.0 equiv) and CsCl (5.0 equiv) in CDCl$_3$. The asterisk denotes a residual NMR solvent peak.
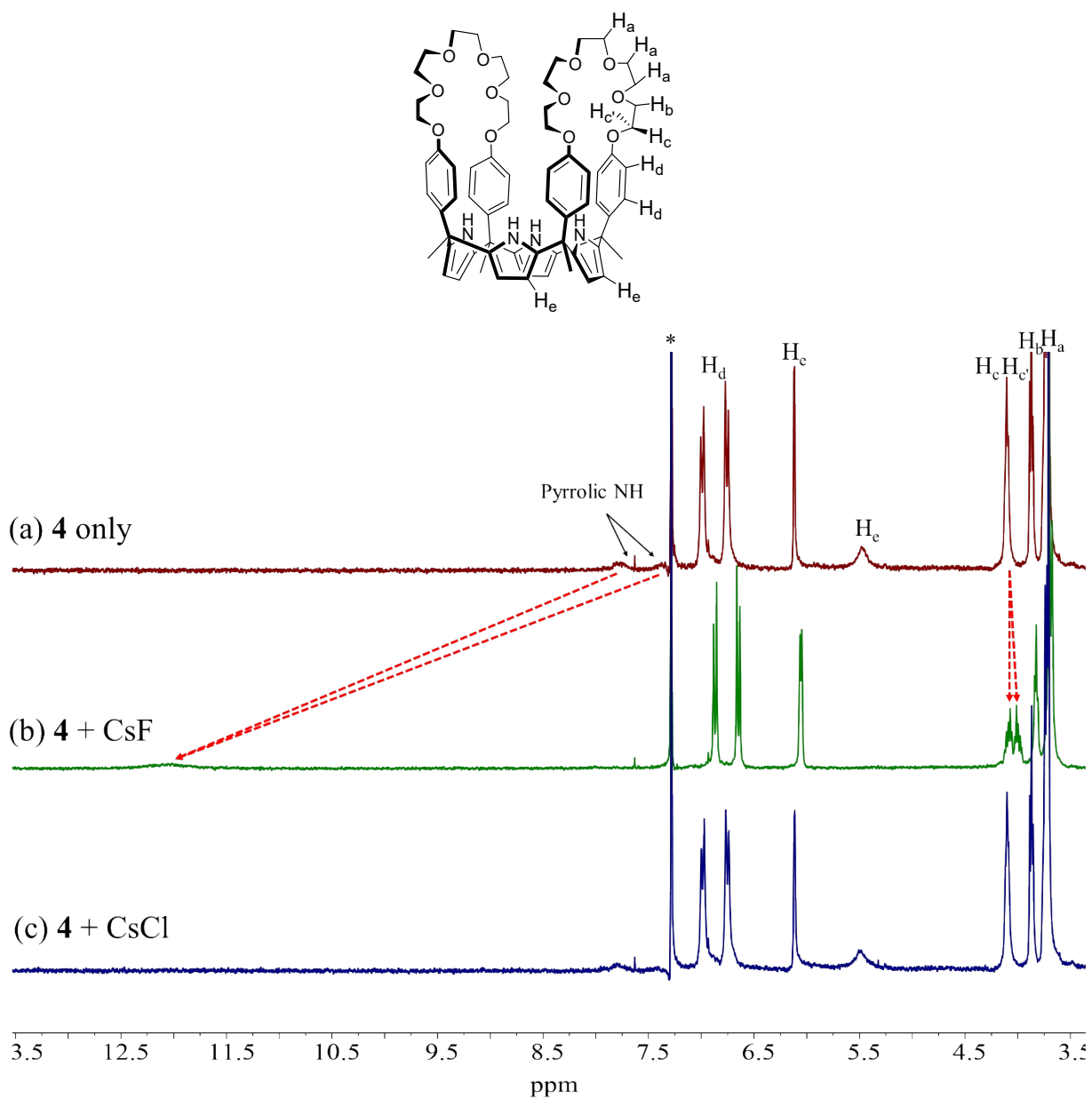
Fig. S26 Partial ^{1}H NMR spectra (300 MHz, 25 °C) of receptor **4** (3 mM) before and after the addition of solid CsF (5.0 equiv) and CsCl (5.0 equiv) in CDCl$_3$. The asterisk denotes a residual NMR solvent peak.

.
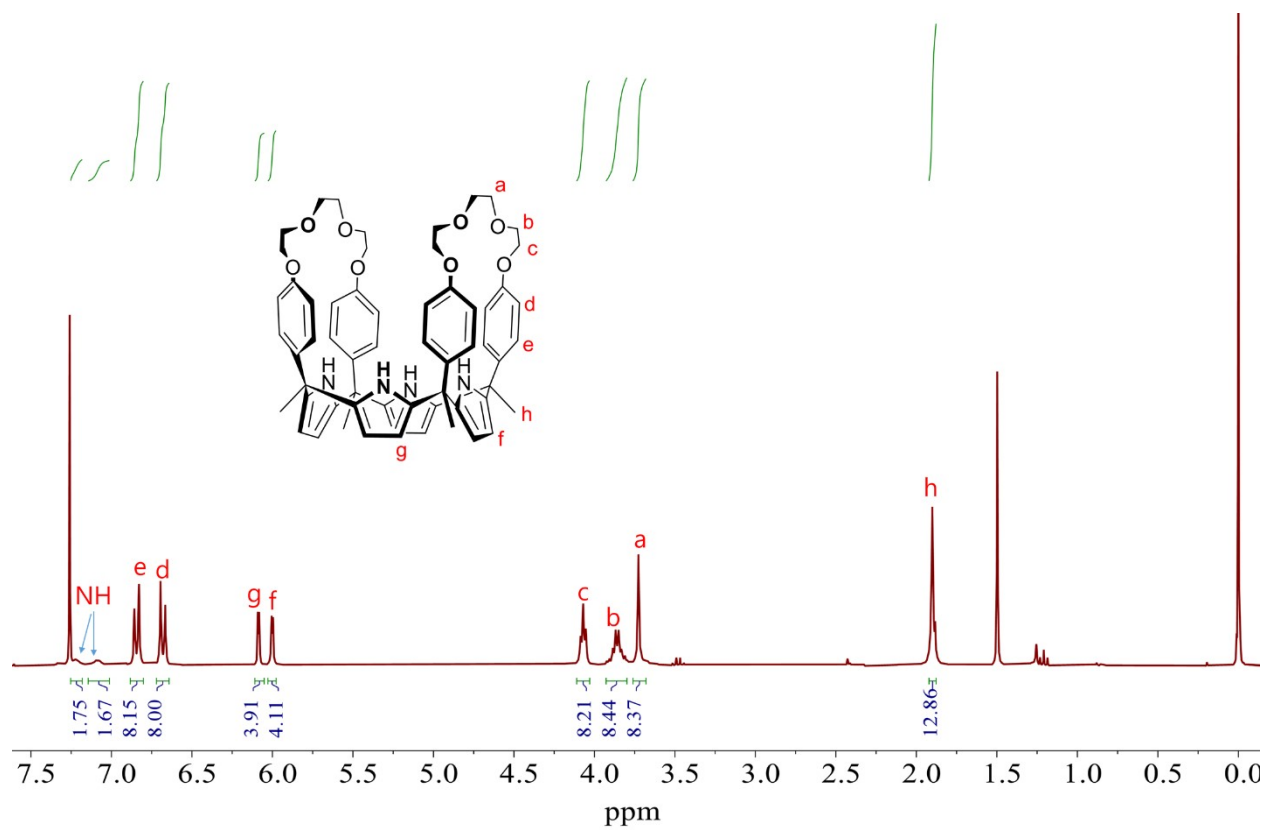
Fig. S27 ^{1}H NMR spectrum of **2** recorded in CDCl$_3$.
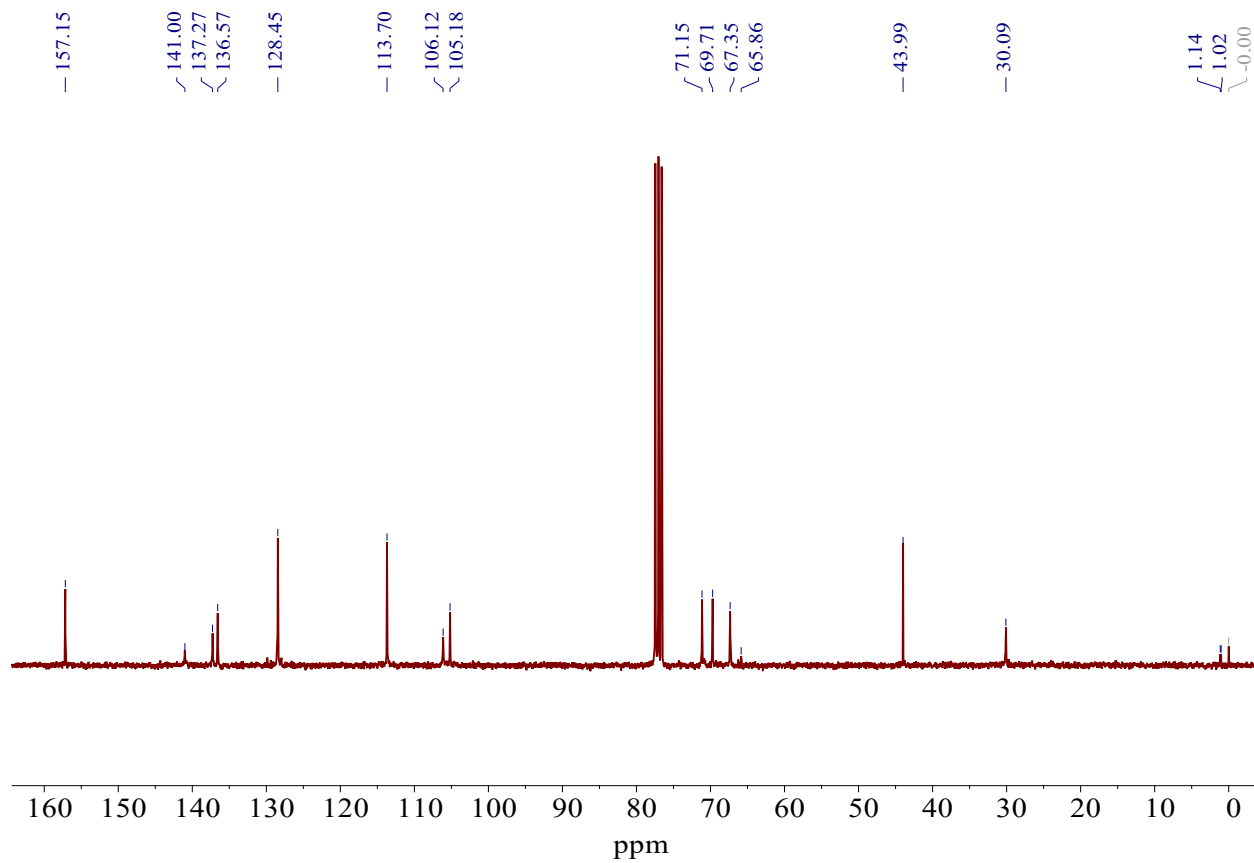
Fig. S28 ^{13}C NMR spectrum of **2** recorded in CDCl$_3$.
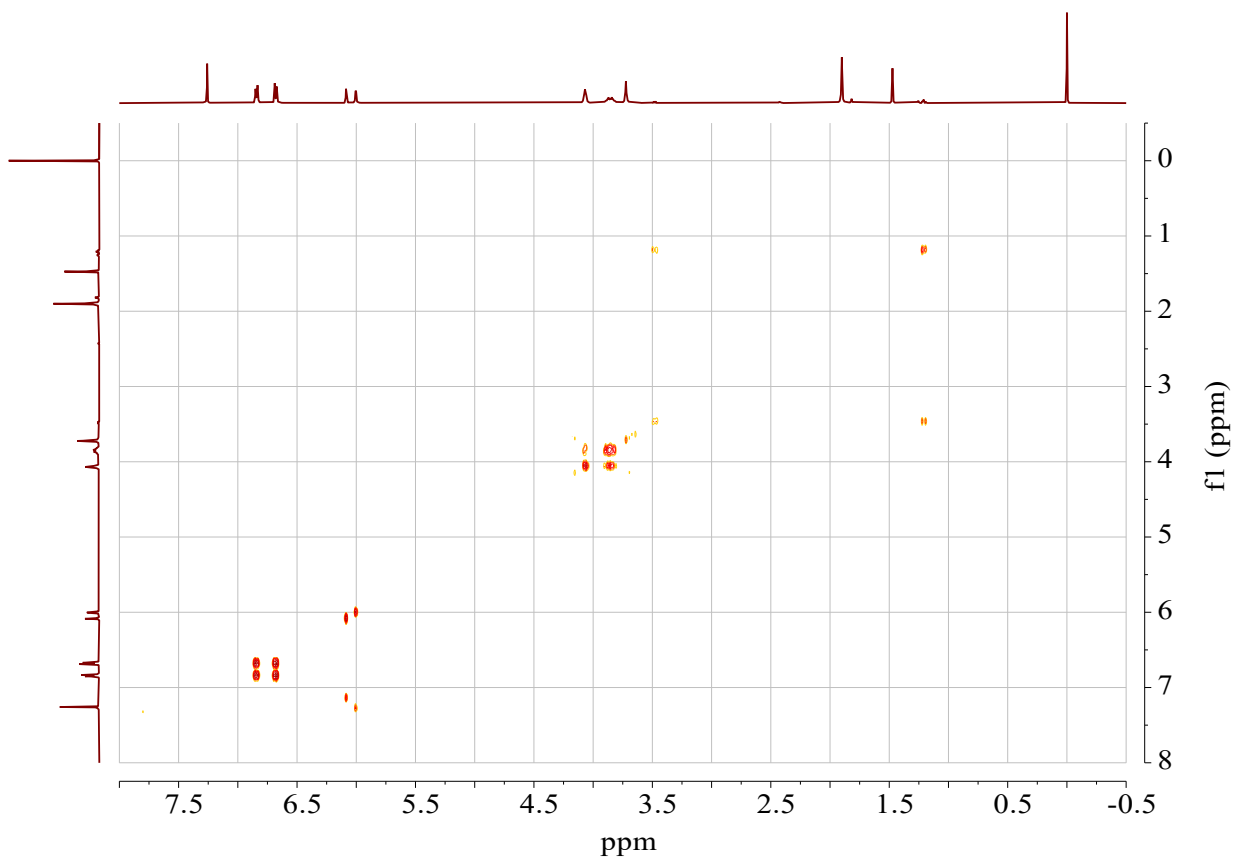
Fig. S29 H-H COSY NMR spectrum (300 MHz, 25 °C) of **2** in CDCl3.
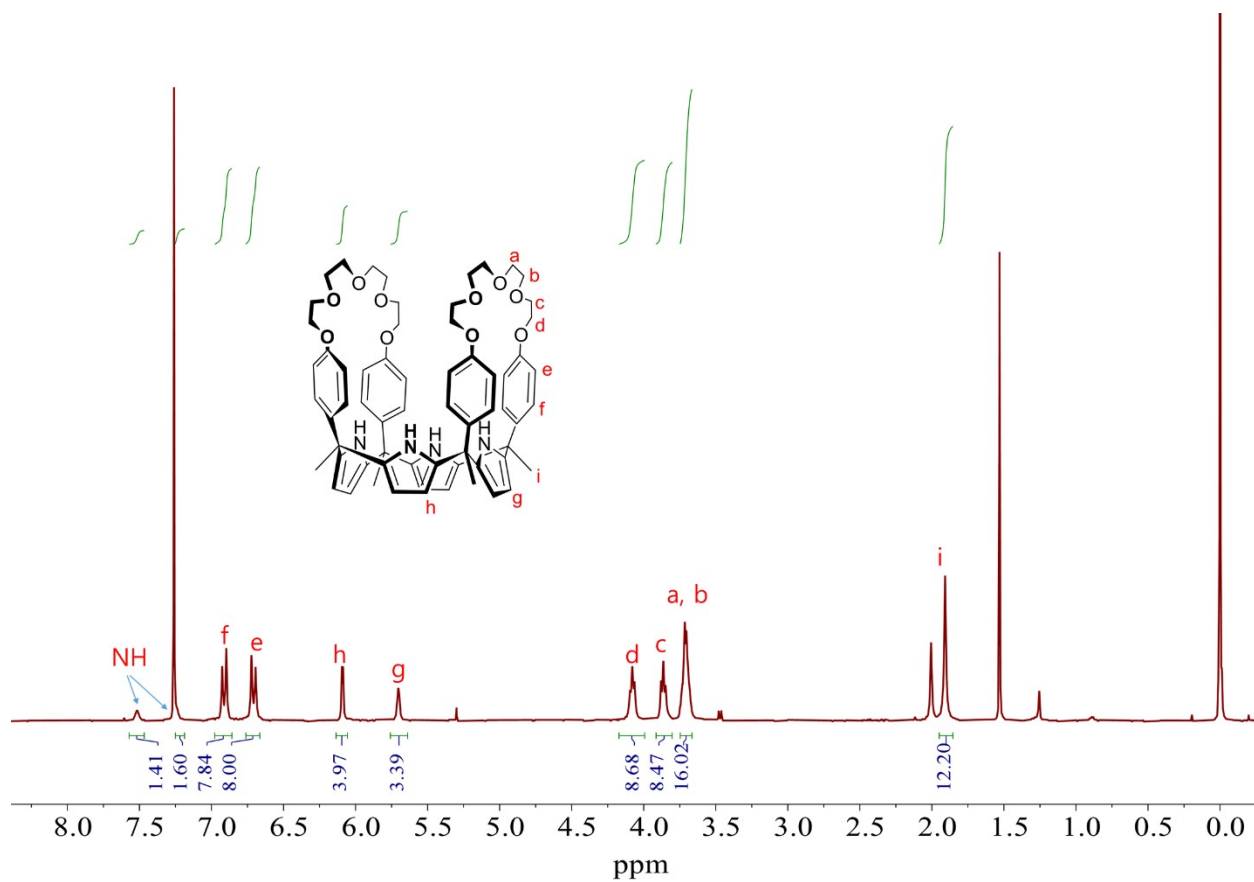
Fig. S30 ¹H NMR spectrum of **3** recorded in CDCl₃.
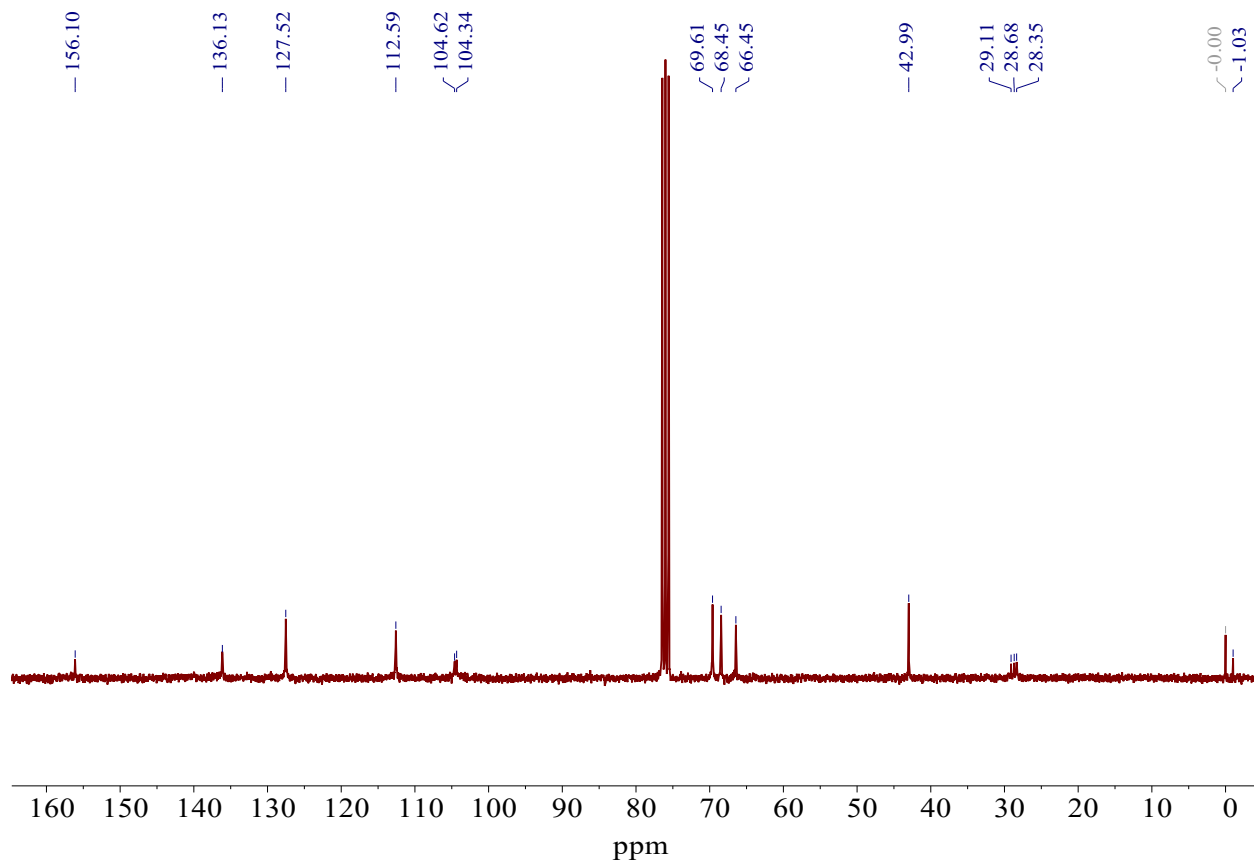
Fig. S31 ¹³C NMR spectrum of **3** recorded in CDCl₃.
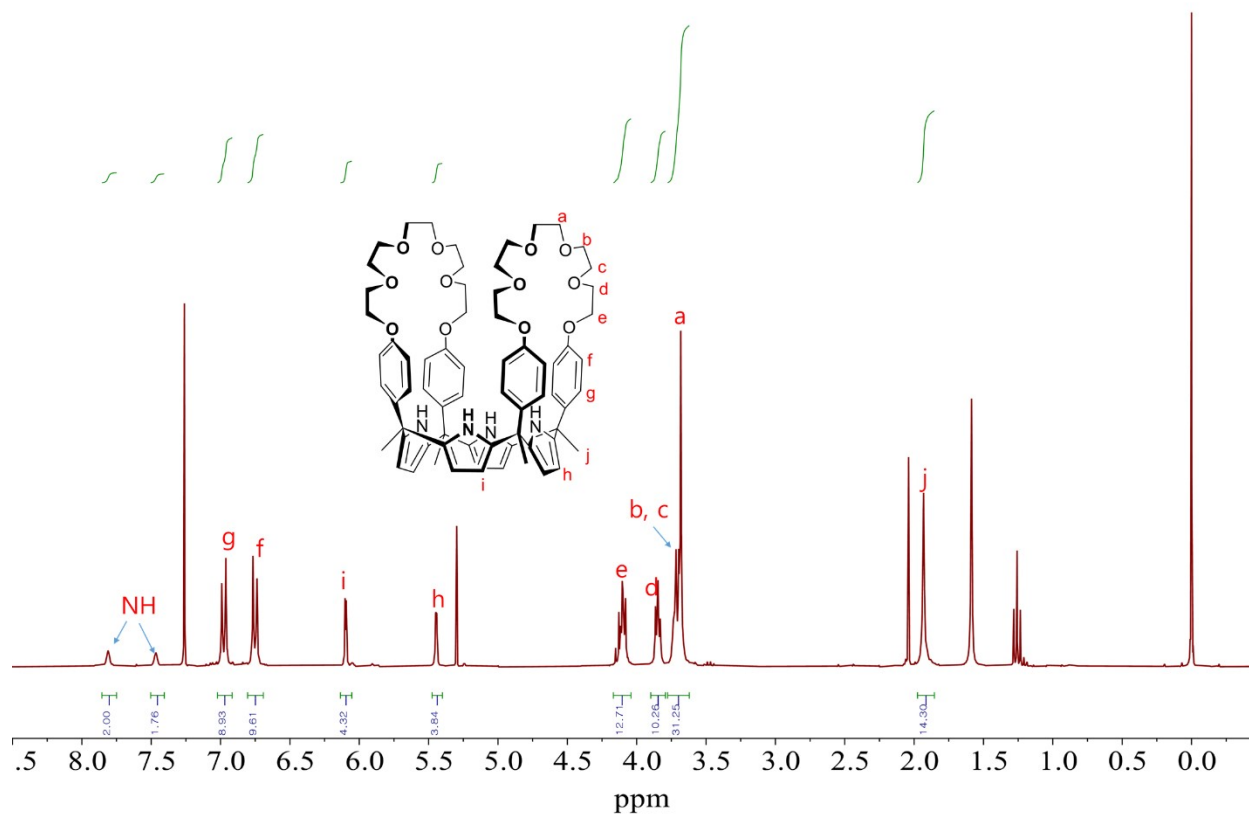
Fig. S32 ^{1}H NMR spectrum of **4** recorded in CDCl₃.
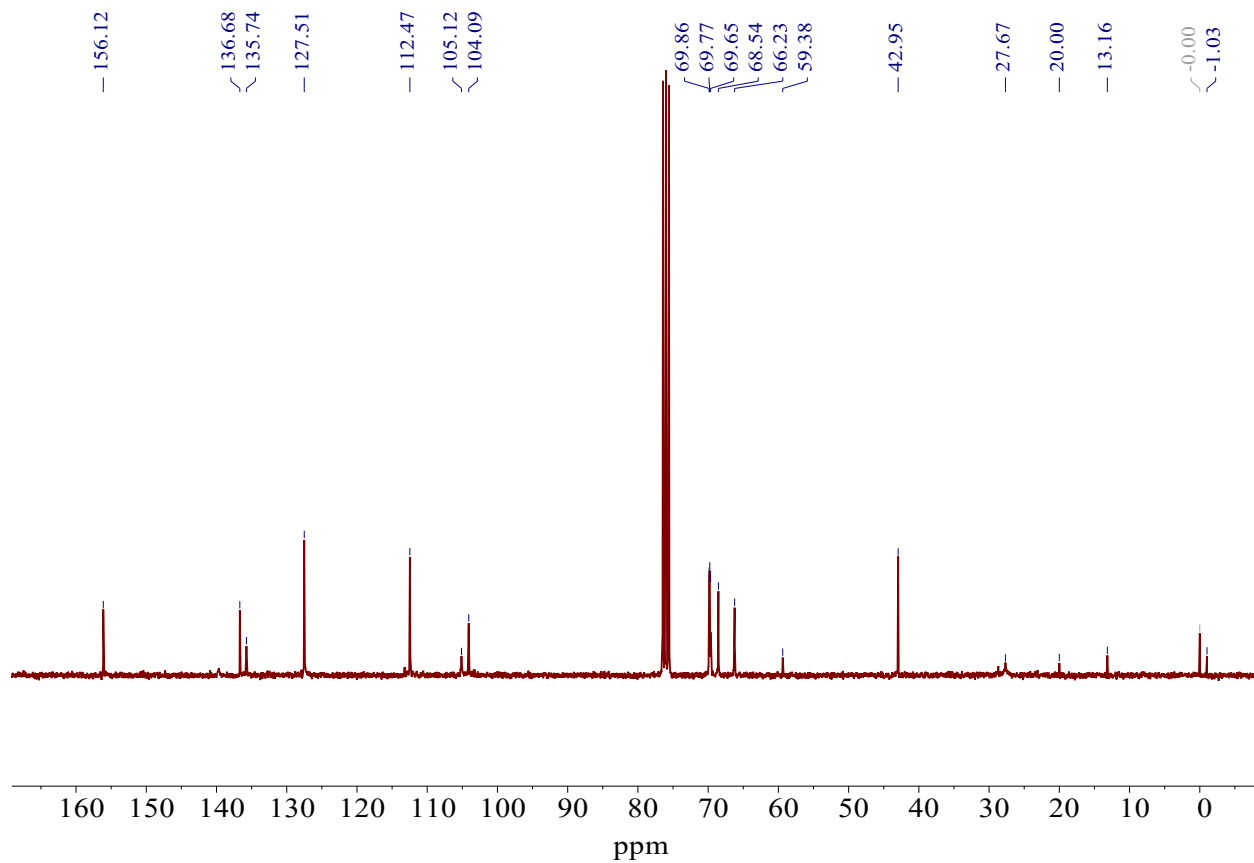
Fig. S33 ^{13}C NMR spectrum of **4** recorded in CDCl$_3$.

```
Data : YJH-C4P CE4_HR      Date : 24-Jan-2021 14:59
Instrument :  MStation
Sample : -
Note : -
Inlet : Direct      Ion Mode : FAB+
RT : 3.40 min      Scan# : 52
Elements : C 100/1, H 100/1, N 8/1, O 8/1
Mass Tolerance     : 1000ppm, 3mmu if m/z > 3
Unsaturation (U.S.) : -0.5 - 31.0


     Observed m/z    Int%      Err[ppm / mmu]    U.S.  Composition
   1   969.4825      7.87       +2.3 /  +2.3     30.5  C60 H65 N4 O8
```

Fig. S34 HR FAB mass data of **2**.

Single Mass Analysis
Tolerance = 50.0 PPM / DBE: min = -30.0, max = 80.0
Element prediction: Off
Number of isotope peaks used for i-FIT = 5
Monoisotopic Mass, Even Electron Ions
334 formula(e) evaluated with 21 results within limits (up to 5 closest results for each mass)
Elements Used:

Mass	Calc. Mass	mDa	PPM	DBE	Formula		i-FIT	i-FIT Norm	Fit Conf %	C	H	N	O
969.4792	969.4784	0.8	0.8	43.5	C72 H61 N2 O		153.8	3.428	3.24	72	61	2	1
	969.4802	-1.0	-1.0	30.5	C60 H65 N4 O8		151.3	0.842	43.09	60	65	4	8
	969.4744	4.8	5.0	39.5	C67 H61 N4 O3		152.9	2.503	8.18	67	61	4	3
	969.4843	-5.1	-5.3	34.5	C65 H65 N2 O6		152.5	2.062	12.72	65	65	2	6
	969.4690	10.2	10.5	30.5	C61 H65 N2 O9		151.5	1.116	32.76	61	65	2	9
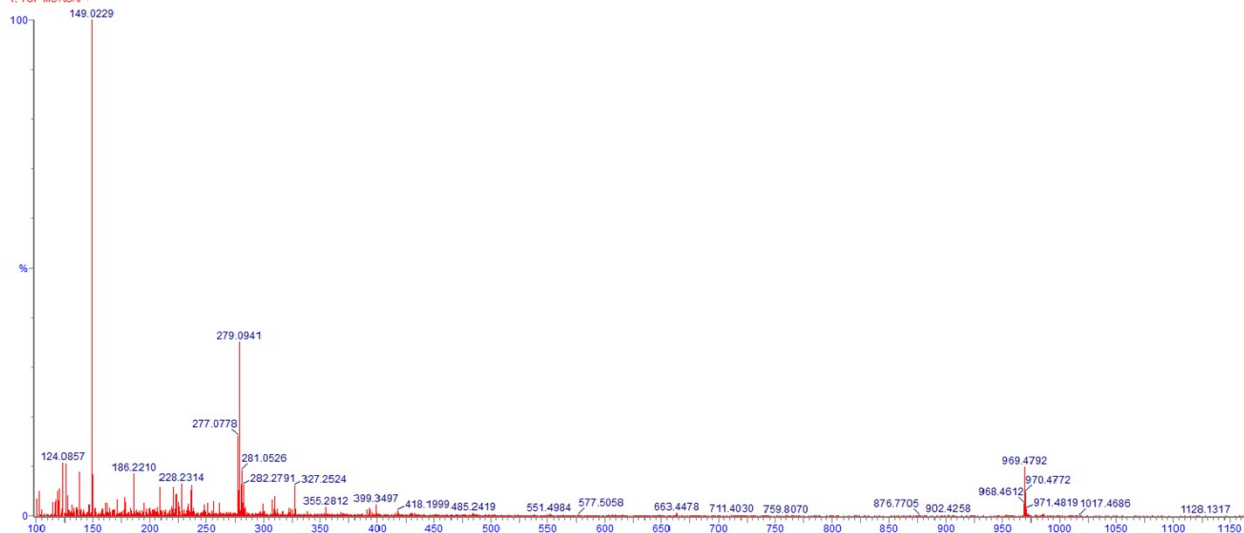
Fig. S35 HR ESI mass spectrum of **2**.

```
Data : YJH-C4P CE5_HR      Date : 26-Jan-2021 16:04
Instrument :  MStation
Sample : -
Note : -
Inlet : Direct      Ion Mode : FAB+
RT : 4.40 min      Scan# : 67
Elements : C 100/1, H 100/1, N 4/1, O 10/1
Mass Tolerance    : 1000ppm, 3mmu if m/z > 3
Unsaturation (U.S.) : -0.5 - 35.0


      Observed m/z    Int%      Err[ppm / mmu]    U.S.  Composition
   1   1057.5326    13.21       -0.1 /  -0.1     30.5   C64 H73 N4 O10
```

Fig. S36 HR FAB mass data of **3**.
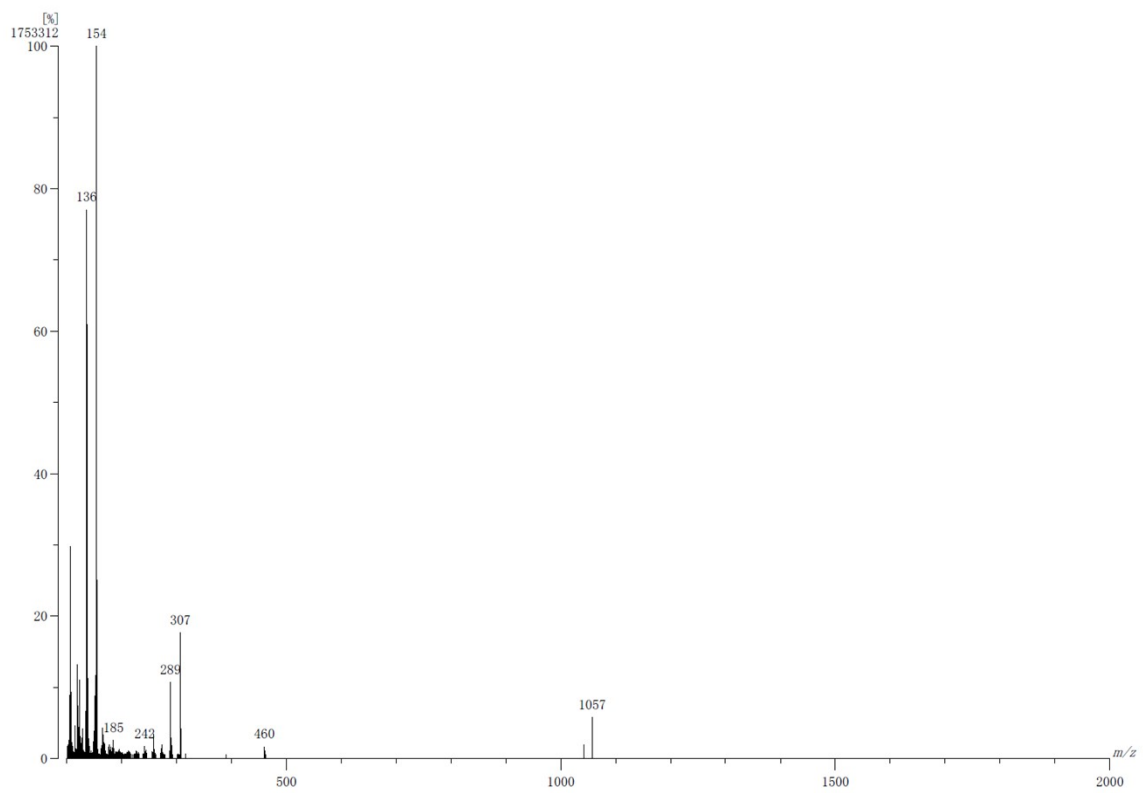
Fig. S37 FAB mass spectrum of compound **3**.

```
Data : YJH-C4P CE6_HR        Date : 26-Jan-2021 16:29
Instrument :  MStation
Sample : -
Note : -
Inlet : Direct       Ion Mode : FAB+
RT : 2.47 min        Scan# : 38
Elements : C 100/1, H 100/1, N 4/1, O 12/1
Mass Tolerance      : 1000ppm, 3mmu if m/z > 3
Unsaturation (U.S.) : -0.5 - 35.0


        Observed m/z    Int%      Err[ppm / mmu]    U.S.  Composition
    1    1145.5830      9.86       -1.8 /  -2.1     30.5  C68 H81 N4 O12
```

Fig. S38 HR FAB mass data of **4**.

Mass	RA	Calc. Mass	mDa	PPM	DBE	Formula				i-FIT	i-FIT Norm	Fit Conf %	C	H	N	O
1145.5840	100.00	1145.5851	-1.1	-1.0	30.5	C68 H81 N4 O12				495.9	0.312	73.23	68	81	4	12
		1145.5806	3.4	3.0	39.0	C77 H79 N O8				499.9	4.280	1.38	77	79	1	8
		1145.5792	4.8	4.2	39.5	C75 H77 N4 O7				498.7	3.111	4.46	75	77	4	7
		1145.5891	-5.1	-4.5	34.5	C73 H81 N2 O10				498.3	2.690	6.79	73	81	2	10
		1145.5765	7.5	6.5	35.0	C72 H79 N3 O10				497.5	1.956	14.14	72	79	3	10

Fig. S39 HR ESI mass spectrum of compound **4**

4. X-ray crystal data

Table S1.   Crystal data and structure refinement for **2**·MeOH.

Identification code	**2**·MeOH
Empirical formula	C63 H69 Cl6 N4 O9
Formula weight	1238.92
Temperature	173(2) K
Wavelength	0.71073 Å
Crystal system	Orthorhombic
Space group	Pnma
Unit cell dimensions	a = 20.3119(4) Å a= 90°.
	b = 21.5671(5) Å b= 90°.
	c = 14.0259(3) Å g = 90°.
Volume	6144.3(2) Å^3
Z	4
Density (calculated)	1.339 Mg/m^3
Absorption coefficient	0.339 mm^{-1}
F(000)	2596
Crystal size	0.282 x 0.258 x 0.203 mm^3
Theta range for data collection	1.732 to 28.303°.
Index ranges	-27<=h<=27, -28<=k<=28, -18<=l<=18
Reflections collected	97609
Independent reflections	7836 [R(int) = 0.0695]
Completeness to theta = 25.242°	100.0 %
Absorption correction	Semi-empirical from equivalents
Max. and min. transmission	0.7457 and 0.7131
Refinement method	Full-matrix least-squares on F^2
Data / restraints / parameters	7836 / 0 / 397
Goodness-of-fit on F^2	1.049
Final R indices [I>2sigma(I)]	R1 = 0.0919, wR2 = 0.2701
R indices (all data)	R1 = 0.1351, wR2 = 0.3085
Extinction coefficient	n/a
Largest diff. peak and hole	2.261 and -1.748 e.Å^{-3}
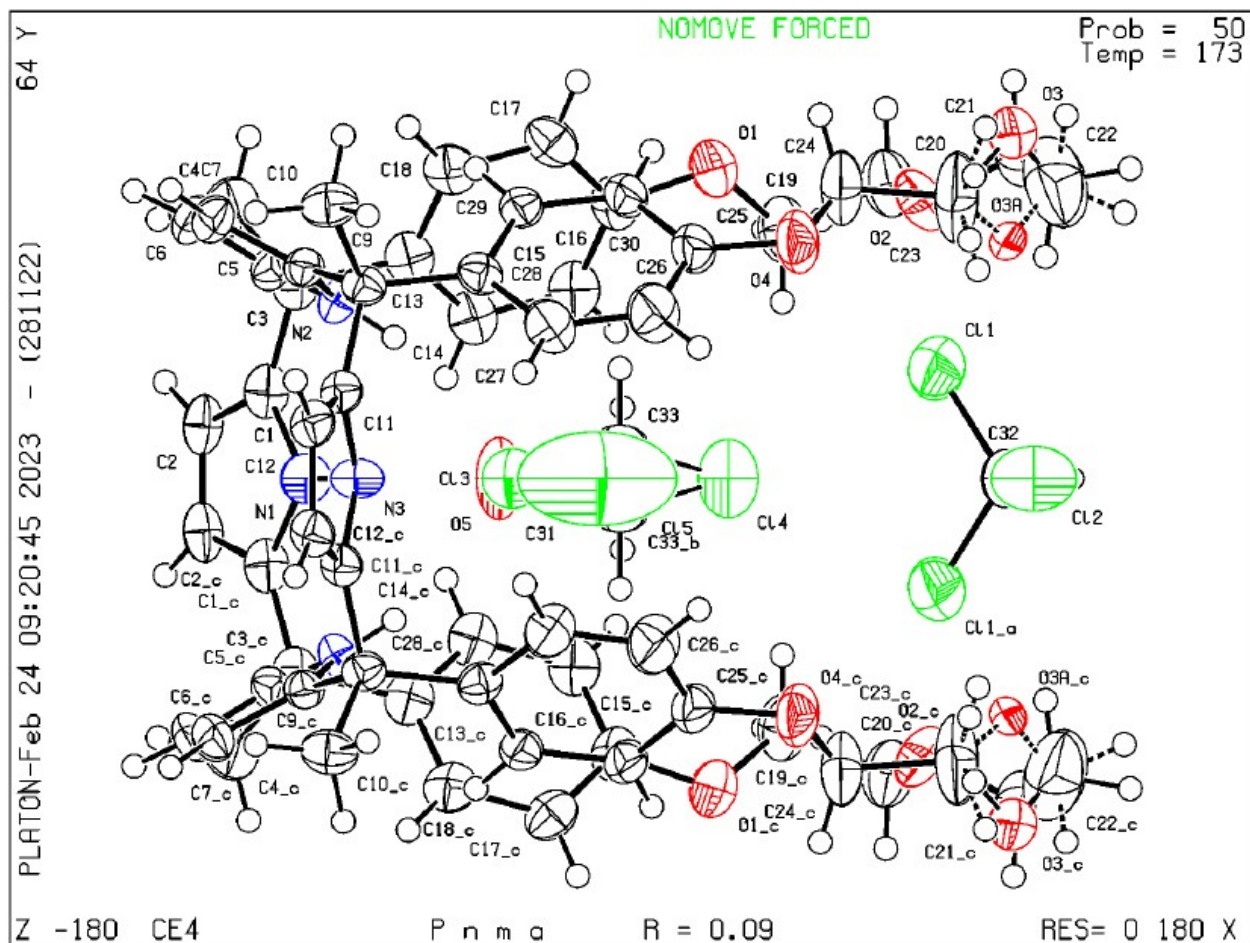
Fig. S40 View of **2**·MeOH complex. Displacement ellipsoids are scaled to the 50% probability level.

X-ray Experimental for 3·Na⁺: Crystals grew as clusters of thin, colorless plates by vapor diffusion of methanol/ethanol into a chloroform solution. The data crystal was cut from a larger crystal and had approximate dimensions; 0.29 x 0.19 x 0.050 mm. The data were collected on a Rigaku Oxford Diffraction HyPix6000E Dual Source diffractometer using a μ-focus Cu Kα radiation source (λ = 1.5418Å) with collimating mirror monochromators. A total of 3508 frames of data were collected using ω-scans with a scan range of 0.5° and a counting time of 6.6 seconds per frame for frames collected with a detector offset of +/- 48.7° and 26.3 seconds per frame with frames collected with a detector offset of +/- 107.8°. The data were collected at 100 K using an Oxford Cryostream low temperature device. Details of crystal data, data collection and structure refinement are listed in Table S2. Data collection, unit cell refinement and data reduction were performed using Rigaku Oxford Diffraction's CrysAlisPro V 1.171.42.25a.[3] The structure was solved by direct methods using SHELXT[4] and refined by full-matrix least-squares on F^2 with anisotropic displacement parameters for the non-H atoms using SHELXL-2018/3.[5] Structure analysis was aided by use of the programs PLATON[6] and OLEX2.[7] The hydrogen atoms on the carbon atoms were calculated in ideal positions with isotropic displacement parameters set to 1.2xUeq of the attached atom (1.5xUeq for methyl hydrogen atoms).

There was quite a bit of disordered solvent of various components. Both molecules of chloroform were disordered. H-bonded to the pyrrole groups was a mixture of acetone and ethanol. In the interior of the macrocycle was a disordered mixture of methanol and water molecules H-bound to one of the polyether groups. The H atoms on some of the oxygen atoms of the methanol and ethanol molecules could not be adequately modeled and were not included in the final refinement model.

The function, $\Sigma w(|F_o|^2 - |F_c|^2)^2$, was minimized, where $w = 1/[(\sigma(F_o))^2 + (0.0789*P)^2 + (3.0482*P)]$ and $P = (|F_o|^2 + 2|F_c|^2)/3$. $R_w(F^2)$ refined to 0.153, with R(F) equal to 0.0563 and a goodness of fit, S, = 1.05. Definitions used for calculating R(F), $R_w(F^2)$ and the goodness of fit, S, are given below.[8] The data were checked for secondary extinction but no correction was necessary. Neutral atom scattering factors and values used to calculate the linear absorption coefficient are from the International Tables for X-ray Crystallography (1992).[9] All figures were generated using SHELXTL/PC.[10] Tables of positional and thermal parameters, bond lengths and angles, torsion angles and figures may be found from the Cambridge Crystallographic Centre by referencing CCDC number 2258328.

Table S2.   Crystal data and structure refinement for **3**·Na$^+$.

Empirical formula	C71.81 H93 Cl7 N4 Na O19
Formula weight	1587.30
Temperature	100.03(12) K
Wavelength	1.54184 Å
Crystal system	triclinic
Space group	P -1
Unit cell dimensions	a = 14.2739(3) Å a= 110.4157(8)°.
	b = 15.65634(16) Å b= 90.9004(15)°.
	c = 19.10054(13) Å g = 103.4262(16)°.
Volume	3869.11(10) Å^3
Z	2
Density (calculated)	1.362 Mg/m^3
Absorption coefficient	2.988 mm^{-1}
F(000)	1668
Crystal size	0.29 x 0.19 x 0.05 mm^3
Theta range for data collection	2.482 to 77.374°.
Index ranges	-18<=h<=18, -19<=k<=19, -23<=l<=23
Reflections collected	28080
Independent reflections	28080 [R(int) = ?]
Completeness to theta = 67.684°	99.4 %
Absorption correction	Semi-empirical from equivalents
Max. and min. transmission	1.00000 and 0.67027
Refinement method	Full-matrix least-squares on F^2
Data / restraints / parameters	28080 / 1061 / 1150
Goodness-of-fit on F^2	1.023
Final R indices [I>2sigma(I)]	R1 = 0.0563, wR2 = 0.1506
R indices (all data)	R1 = 0.0593, wR2 = 0.1529
Extinction coefficient	n/a
Largest diff. peak and hole	0.668 and -0.692 e.Å^{-3}
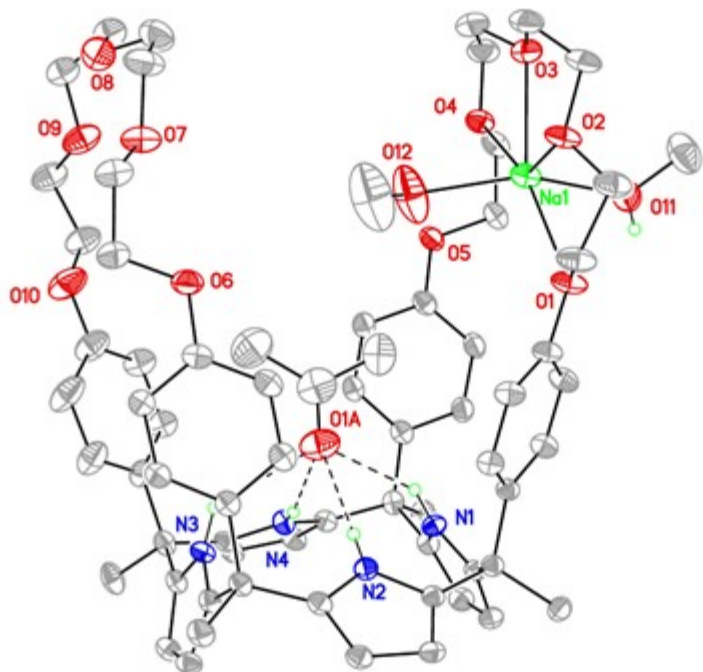
Fig. S41 View of the Na⁺ ion complex in **3** showing the heteroatom labeling scheme. Displacement ellipsoids are scaled to the 50% probability level.   Dashed lines are indicative of a H-bonding interaction.   Most H atoms were omitted for clarity.

5. References

1. P. Anzenbacher, K. Jursíková, V. M. Lynch, P. A. Gale, J. L. Sessler, *J. Am. Chem. Soc.*, 1999, **121**, 11020-11021.

2. J. Aguilera-Sigalat, C. S. de Pipaon, D. Hernandez-Alonso, E. C. J. R. Escudero-Adan, Galan-Mascaros, P. Ballester, *Cryst. Growth Des.*, 2017, **17**, 1328– 1338.

3. CrysAlisPro. Rigaku Oxford Diffraction, HyPix6000E System, CrysAlisPro Software System, 1.171.42.25a.

4. G. M. Sheldrick. *Acta Cryst.*, 2015, **A71**, 3-8.

5. G. M. Sheldrick, (2015). *Acta Cryst.*, 2015, **C71**, 3-8.

6. A. L. Spek, *Acta Cryst.*, 2009, **D65**, 148-155.

7. O. V. Dolomanov, L. J. Bourhis, R. J. Gildea, J. A. K. Howard, and H. Puschmann, *J. Appl. Cryst.*, 2009, **42**, 339-341.

8. $R_w(F^2) = \{\Sigma w(|F_O|^2 - |F_c|^2)^2 / \Sigma w(|F_O|)^4\}^{1/2}$ where w is the weight given each reflection.

    $R(F) = \Sigma (|F_O| - |F_c|) / \Sigma |F_O|\}$ for reflections with $F_O > 4(\sigma(F_O))$.

    $S = [\Sigma w(|F_O|^2 - |F_c|^2)^2 / (n - p)]^{1/2}$, where n is the number of reflections and p is the number of refined parameters.

9. International Tables for X-ray Crystallography (1992). Vol. C, Tables 4.2.6.8 and 6.1.1.4, A. J. C. Wilson, editor, Boston: Kluwer Academic Press.

10. Sheldrick, G. M. (1994). SHELXTL/PC (Version 5.03). Siemens Analytical X-ray Instruments, Inc., Madison, Wisconsin, USA.